

MULTI-SEGMENT CONTINUOUS CABLES WITH FRICTIONAL CONTACT  
ALONG THEIR SPAN

A THESIS SUBMITTED TO  
THE GRADUATE SCHOOL OF NATURAL AND APPLIED SCIENCES  
OF  
MIDDLE EAST TECHNICAL UNIVERSITY

BY  
ABDULLAH DEMİR

IN PARTIAL FULFILLMENT OF THE REQUIREMENTS  
FOR  
THE DEGREE OF DOCTOR OF PHILOSOPHY  
IN  
CIVIL ENGINEERING

JULY 2017



Approval of the thesis:

**MULTI SEGMENT CONTINUOUS CABLES WITH FRICTIONAL  
CONTACT ALONG THEIR SPAN**

Submitted by **ABDULLAH DEMİR** in partially fulfillment of the requirements of the degree of **Philosophy of Doctoral in Civil Engineering Department Middle East Technical University** by,

Prof. Dr. Gülbin Dural Ünver  
Dean, Graduate School of **Natural and Applied Sciences**

Prof. Dr. İsmail Özgür Yaman  
Head of Department, **Civil Engineering**

Assoc. Prof. Dr. M. Uğur Polat  
Supervisor, **Civil Engineering Dept., METU**

**Examining Committee Members:**

Prof. Dr. Mehmet Utku  
Dept. of Civil Engineering, METU

Prof. Dr. Suha Oral  
Dept. of Mechanical Engineering, METU

Assoc. Prof. Dr. M. Uğur Polat  
Dept. of Civil Engineering, METU

Prof. Dr. Mustafa Şahmaran  
Dept. of Civil Engineering, Hacettepe University

Assoc. Prof. Dr. Ahmet Hakan Argeşo  
Dept. of Manufacturing Engineering, Atılım University

**Date:** \_\_\_\_\_

**I hereby declare that all information in this document has been obtained and presented in accordance with academic rules and ethical conduct. I also declare that, as required by these rules and conduct, I have fully cited and referenced all material and results that are not original to this work.**

Name, Last name: Abdullah Demir

Signature :

## **ABSTRACT**

### **MULTI-SEGMENT CONTINUOUS CABLES WITH FRICTIONAL CONTACT ALONG THEIR SPAN**

Demir, Abdullah

Ph.D. in Department of Civil Engineering

Supervisor: Assoc. Prof. Dr. Mustafa Uğur Polat

July 2017; 90 pages

Cables are highly nonlinear structural members under transverse loading. This nonlinearity is mainly due to the close relationship between the final geometry under transverse loads and the resulting stresses in its equilibrium state rather than the material properties. In practice, the cables are usually utilized as isolated single-segment elements fixed at the ends. Various studies and solution procedures suggested by researchers are available in the literature for such isolated cables. However, not much work is available for multi-segment continuous cables with multiple intermediate supports between its two ends.

In this thesis, a solution procedure based on contact mechanics is proposed for the non-linear interaction between a multi-segment continuous cable and an elastic structure such as a plane truss. The intermediate supports represent the target nodal points of the structure where the cable is likely to come into contact with the structure. Therefore, the intermediate supports of the multi-segment continuous cable are assumed to be frictional and elastic. Moreover, the cables are not constrained to be in contact with each of these target supports. Actual support locations along the cable are determined in the course of the iterative non-linear analysis.

A cable and a bar element are formulated mathematically with their geometric nonlinearities. The coupling is established and non-linear interaction between the two structures is determined by the principles of contact mechanics. Proposed mathematical model is coded and verification analyses are done with a sample model composed of a cable and a truss structure. A number of case studies are carried out for a real-life application of truss structures post-tensioned by a continuous cable.

Keywords: cable, structural cable, multi-segment continuous cable, contact mechanics, continuous cable with multiple supports

## ÖZ

### AÇIKLIĞI BOYUNCA SÜRTÜNMELİ KONTAK HALİNDEKİ ÇOK AÇIKLIKLI SÜREKLİ KABLOLAR

Demir, Abdullah

Doktora, İnşaat Mühendisliği Bölümü

Tez Yöneticisi: Doç. Dr. Mustafa Uğur Polat

Temmuz 2017; 90 Sayfa

Kablolar eksenine dik yükler altında son derecede doğrusal olmayan davranış gösterirler. Bunun nedeni kablonun malzeme davranışından ziyade kablonun böyle bir yük altındaki son konumu ve dolayısı ile oluşan gerilmeler ile uygulanan yük arasındaki yakın ilişkidir. Uygulamada kablolar daha çok iki ucu sabit tek parça eleman olarak kullanılır. Literatürde böyle bir kullanım durumunda kablonun analizi için araştırmacılar tarafından önerilen değişik yaklaşımlar mevcuttur. Ancak iki ucu arasında bazı ara noktalarda da mesnetlenen çok parçalı sürekli kablolar için fazlaca bir çalışma bulunmamaktadır.

Bu tezde, çok parçalı bir kablonun düzlem kafes kiriş gibi elastik bir başka yapı ile doğrusal olmayan etkileşimi için kontak mekanik prensiplerine dayanan bir çözüm yöntemi önerilmektedir. Çok parçalı kablonun ara mesnetleri kablonun yapısal sistem ile temas oluşturacağı olası kontak noktalarını temsil etmektedir. Dolayısı ile kablo boyunca ara mesnetler sürtünmeli ve elastik olarak kabul edilmektedir. Ayrıca kablo doğrusal olmayan analiz sürecinin her aşamasında yapısal sistem üzerinde seçilen olası kontak noktaları ile kontak halinde olmaya da zorlanmamaktadır. Kablo boyunca

elastik yapısal sistem ile oluşacak kontak noktaları olan ara mesnetlerin gerçek konumları doğrusal olmayan artımsal ve iteratif analiz sürecinde belirlenmektedir.

Bu amaçla matematiksel olarak formüle edilen bir kablo ve bir çubuk elemanı kullanılarak yapısal sistem ile kablo modellendikten sonra kablo ile yapısal sistemin kuplajı ve iki yapı arasındaki doğrusal olmayan etkileşim kontak mekanik prensipleri bazında belirlenmektedir. Önerilen yöntem için oluşturulan bir bilgisayar yazılımı kullanılarak yöntemin verifikasyonu kablo ve kafes giriş sistemden oluşan örnek problemlerle yapılmıştır. Yöntem ard germeli kafes giriş sistem gibi pratik uygulama örnekleri ile de test edilmektedir.

Anahtar Kelimeler: kablo, yapısal kablo, çok açıklıklı sürekli kablo, kontak mekanik, çok mesnetli sürekli kablo



**To My Family**

## TABLE OF CONTENTS

ABSTRACT .....	v
ÖZ.....	vii
TABLE OF CONTENTS .....	x
LIST OF TABLES .....	xiii
LIST OF FIGURES.....	xiv
1. INTRODUCTION .....	1
1.1 General.....	1
1.2 Purpose .....	2
1.3 Previous Studies .....	3
1.3.1 Studies on Cables .....	3
1.3.2 Studies on Contact Mechanics .....	5
2. FORMULATION OF GEOMETRICALLY NONLINEAR BAR ELEMENT ...	7
2.1 General.....	7
2.2 Updated Lagrangian Formulation.....	7
2.2.1 Formulation of Truss Element.....	9
3. SINGLE AND MULTI-SEGMENT CABLE.....	13
3.1 Single-Segment Cable Analysis .....	13
3.1.1 Cable Equilibrium Equations .....	13

3.1.2	Stiffness Matrix .....	15
3.1.3	Newton-Raphson Method .....	20
3.2	Multi-Segment Cable Analysis .....	21
3.2.1	Direct Stiffness Approach .....	22
3.2.2	Tension Distribution Method (Relaxation Method).....	25
4.	CONTACT MECHANICS .....	27
4.1	General .....	27
4.2	Potential of Sticking Contact.....	29
4.3	Potential of Sliding Contact .....	32
4.4	Governing Finite Element Equations .....	33
4.5	Governing Finite Element Equations in Local Coordinates.....	36
4.6	Contact Conditions .....	38
4.6.1	Contact Search Algorithm.....	38
4.6.2	Contact Type Algorithm .....	40
5.	SOLUTION PROCEDURE.....	43
5.1	General .....	43
5.2	Governing Set of Equations .....	43
5.3	Solution Procedure .....	44
6.	VERIFICATION AND VALIDATION OF PROPOSED ALGORITHM .....	51
6.1	General .....	51
6.2	Verification Test Structure .....	51

6.2.1	Initial Configuration of Cable .....	52
6.2.2	Frictional Environment .....	59
6.2.3	Altered Cable Lengths.....	62
7.	CASE STUDIES .....	65
7.1	General.....	65
7.2	Description of the Sample Truss Structure.....	65
7.2.1	Original Design of the Truss Structure .....	66
7.2.2	Case I: Internal Post-tensioning .....	67
7.2.3	Case II: External Post-tensioning with Nearby Anchorage .....	68
7.2.4	Case III External Post-tensioning with Remote Anchorage.....	69
7.3	Discussion on the Results of Case Studies .....	69
8.	SUMMARY AND CONCLUSIONS .....	71
8.1	Summary.....	71
8.2	Conclusions .....	71
	REFERENCES.....	75
	APPENDIX .....	79
	CURRICULUM VITAE .....	89

## LIST OF TABLES

### TABLES

Table 6.1 Structural displacements for frictionless symmetric tensioning .....	54
Table 6.2 Contact forces for frictionless symmetric tensioning .....	54
Table 6.3 Displacements of Node 19 for different number of cable finite elements .	56
Table 6.4 Displacements of node 19 for different maximum allowable error. ....	58
Table 6.5 Displacements of Node 6 for different coefficients of friction .....	59
Table 6.6 Contact forces of Node 6 for different coefficients of friction .....	60
Table 6.7 Displacements of Node 19 for different coefficients of friction .....	60
Table 6.8 Contact forces of Node 19 for different coefficients of friction .....	60
Table 6.9 Displacements of node 14 for different coefficients of friction .....	61
Table 6.10 Contact forces of node 14 for different coefficients of friction .....	61
Table 6.11 Results for different final lengths of cable .....	63
Table 7.1 Circular pipe sections used in the structure .....	66

## LIST OF FIGURES

### FIGURES

Figure 1.1 Contact between cable and elastic structure .....	2
Figure 1.2 Single-segment cable .....	4
Figure 1.3 Multi-segment continuous cable .....	4
Figure 2.1 Deformation of a bar element .....	9
Figure 2.2 Coordinate system of a bar element.....	9
Figure 3.1 Configuration of single-segment cable in space. ....	14
Figure 3.2 Reactions on cable .....	17
Figure 3.3 Newton-Raphson method in schematic form for single-segment cable ...	21
Figure 3.4 Configuration of multi-segment continuous cable.....	22
Figure 3.5 Cable tensions at support $i$ . ....	22
Figure 4.1 Geometry of contact.....	28
Figure 4.2 Contact forces .....	29
Figure 4.3 Geometry of contact in sticking condition.....	31
Figure 4.4 Geometry of contact in sliding condition .....	33
Figure 4.5 Vectors and angles for contact search.....	39
Figure 5.1 Flow diagram of the proposed algorithm.....	46

Figure 5.2 Flow chart for the analysis of the elastic structure .....	47
Figure 5.3 Flow chart for the analysis of cable.....	48
Figure 5.4 Flow chart for contact search.....	49
Figure 6.1 Geometry of the verification model.....	52
Figure 6.2 Initial cable configuration I .....	52
Figure 6.3 Initial cable configuration II .....	53
Figure 6.4 Initial and final geometry of the structure predicted by the proposed procedure.....	55
Figure 6.5 Initial and final geometry of the structure predicted by ANSYS .....	55
Figure 6.6 Displacement in X direction of Node 19 vs. the number of finite elements .....	57
Figure 6.7 Displacement in Y direction of Node 19 vs. the number of finite elements .....	57
Figure 6.8 Displacement in X direction of Node 19 vs. the maximum allowable error. .....	58
Figure 6.9 Displacement in Y direction of Node 19 vs. the maximum allowable error. .....	58
Figure 6.10 Cable tensions vs coefficients of friction.....	62
Figure 6.11 Mid-span displacement vs. final cable length.....	63
Figure 6.12 Cable tension vs. final cable length .....	64
Figure 7.1 Geometry of structure .....	66
Figure 7.2 Geometry of the structure for Case I .....	67

Figure 7.3 Geometry of structure in Case II.....	68
--	----



## **CHAPTER 1**

### **INTRODUCTION**

#### **1.1 General**

Cables are structural elements having negligibly small stiffness in bending and used to span long distances. They are used in cable-stayed bridges, guyed towers, offshore structures, marine vehicles, transmission lines, cable roofs, pre-stressing applications and tensegrity works. Besides, cables are the indispensable elements for tensioning applications.

Basically, if cables are assumed to be weightless and no transverse loading, they are geometrically linear structural elements. Although, this assumption could be valid for cables having smaller cross-sectional areas, there are many applications of cables like suspension bridges where the cables have considerable self-weight and subject to transverse loading. Hence, geometric nonlinearity is the main issue for cable analysis having the effect of its own weight and transverse loading.

Structural cables are usually used in conjunction with some other structural components. Besides its geometric nonlinearity, there is another issue which makes the analysis of cables more troublesome. This is the contact of cables with other structural elements along their span. Depending on the structural design, cables can be fixed at some predefined support locations or slipping might occur on some parts of the structure. In addition, in the course of their loading history, cables can establish contact with some parts of the structure and/or loose contact with some other parts of it. This inherent motion of cable can only be modelled by defining the contact between the cable and the elastic structure, which is the purpose of this thesis.

## 1.2 Purpose

Extensive research have been made for cables passing through the pulleys having predefined location in space. However, pulleys are elastic structural elements and their initial positions can change. Besides, cables can be in contact with structure/pulley or not, depending on many constraints like support conditions, loading regime, the shape of structure, position of contact points and cable length (see Figure 1.1) for both application phase of the cables and the loading phase of the structures. Furthermore, the contact points between cables and the structures can change continuously during loading phase of the application such as post-tensioning of structures.

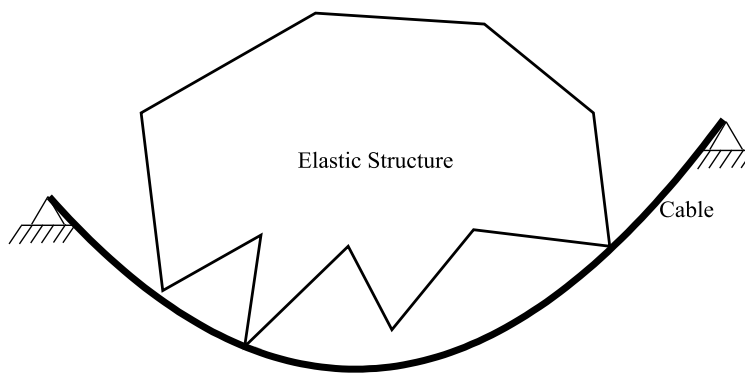


Figure 1.1 Contact between cable and elastic structure

As a result, designing cables with restricted contact points will result in unexpected stress distribution in the post-tensioned structure. Therefore, the contact between the cable and the structure should be modelled without any restriction on the location of contact points to accurately model the interaction between the cable and the structure and obtain a true distribution of stresses. The aim of this thesis is to model the contact between cables and the elastic structures with their inherent motion. A 2D truss system is selected as an elastic structure. A post-tensioning application is modelled for this elastic structure by shortening the continuous cable.

### **1.3 Previous Studies**

Handling of the interaction problem between cables and the structures requires both the non-linear analysis of cables and the mechanics of contact between elastic bodies.. Therefore, the literature is surveyed separately in these two areas.

#### **1.3.1 Studies on Cables**

Cables are non-linear structural elements widely used in many civil engineering applications. The non-linearity is due to their bendable geometry. In other words, cables have nearly zero bending stiffness. Thus, they cannot resist compressive forces. Therefore, cables can be called as tension only members.

In general, cables are composed of many wires. This composition satisfies the condition that, cable has a constant cross-sectional area whereas has a smaller bending stiffness compared with a bar having the same cross sectional area. The most commonly used cables are composed of seven wires, which are called 7-wire strands. There are many types of cables composed of wires and/or strands.

Being a tension only member and having approximately no bending stiffness as explained above, cables are generally used with long geometries supported at both ends. Under these circumstances, cables make sags due to its self-weight. Researchers firstly tried to solve the cable problem by assuming them as weightless and having a parabolic shape. “Equivalent modulus of elasticity approach” is the name of the method proposed by Dischinger (1949). This method was improved by Ernst (1965) with the name; equivalent secant modulus of elasticity approach. Hajdin (1998) summarized the methods. Although, these are old studies, parabolic cable elements were used in recent studies (Ren et al 2008).

The first cable solution considering its self-weight was proposed by Micholas and Brinstiel (1962). Skop and O’Hara made further researches (1970). Peyrot and Goulois (1979) developed a code and verify their proposed method. Polat (1981) uses Newton-Raphson method for nonlinearity in his thesis. Demir (2011) developed the cable element in 3D. There are many other finite element methods proposed by researchers

Fleming (1979), Chue (1983), Wang (1984), Wang et al (1989), Der Kiureghian et al (2005), Andreu et al (2006), Santos et al (2011), Mostafa et al (2013), Ahmadizadeh (2013), Greco et al (2014).

Although the solution of tension only elements have been generally named as cable solution, Demir (2011) proposed an approach for the solution of cables by distinguishing between the two types as single-segment cables (SSC) and multi-segment continuous cables (MSCC). In his description, single-segment cable is a cable with stationary supports at its ends. In contrast, the multi-segment continuous cables are those, which are also supported by some stationary intermediate supports along their span and, over which, they can slip with or without friction. The difference is illustrated in Figure 1.2 and Figure 1.3.

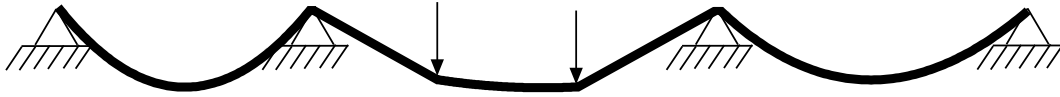


Figure 1.2 Single-segment cable

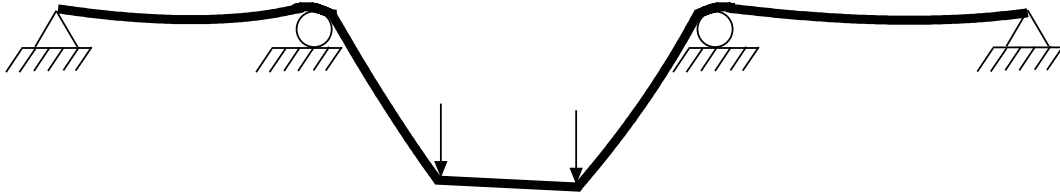


Figure 1.3 Multi-segment continuous cable

Multi-segment cable analysis was first studied by McDonald and Peyrot (1988). Similar studies have been carried out by McDonald and Peyrot (1990), Aufaure (1993), Bruno et al (1999), Aufaure (2000), Zhou et al (2004), Such et al (2009), Impollonia (2011). In these researches, a finite element having three nodes were defined. Thus, cable having three node can satisfy the stress continuity through its geometry. In contrast to these researches, Demir (2011) proposed two methods termed as Direct Stiffness Approach and Tension Distribution Method. Basically, both methods divide the cable into segments (naming whole structure as multi-segment continuous cable)

and search for an equilibrium state satisfying the stress continuity at intermediate roller supports.

In this thesis, a new method based on the principles of contact mechanics is proposed for cables in contact with elastic structures, which can also be called as multi-segment continuous cables in contact with elastic structures. In this new method, the single-segment cable solution proposed by Skop and O'Hara (1970) and reformulated by Demir (2011) is used. This formulation is given in Chapter 3.

In the proposed method of Demir (2011) for multi-segment continuous cables, the cable is forced to pass through the predefined positions of roller supports. In contrast, the method proposed in this thesis establishes a contact between the cable and the elastic structure. Thus, the cable has the ability to establish contact with the elastic structure at some point during the loading phase. It can move together with the elastic structure or make a relative motion without losing its contact. It is not forced to remain in contact throughout the loading history.

### **1.3.2 Studies on Contact Mechanics**

Contact Mechanics is the study of solids in interaction. Interaction is established with the relation between overlap and corresponding forces. As it is known from the mechanics of material, the deformations and the forces are related to each other by the material properties. In addition to the relation in mechanics of materials, the relation between overlaps and the corresponding forces is needed in contact mechanics. This relation can be thought as imposition of constraints.

Imposition of specific displacements on solids can be called as the basis of contact mechanics. The two widely used approaches to constrain the solids are the Lagrange Multiplier Method and the Penalty Method. In these methods, the solids are constrained to have the specified displacements in specified nodes. These constraints are satisfied by defining an additional potential.

In contrast to these methods, in contact mechanics, the solids are free to displace until they touch each other. Although a contact surface is to be defined, solids can be in

contact at any node on defined contact surface. Therefore, contact mechanics can be regarded as the generalized version of Lagrange Multiplier or Penalty approaches.

The research of Hughes et al (1977) is the milestone of the contact mechanics, which bases on their series of reported researches (1974, 1975, 1975). Bathe and Chaudhary published a tidy work (1985) based on researches of Hughes et al (1977). In research of Bathe and Chaudhary (1985) contact mechanics was formulated well for 2D case. This formulation is the basis of the contact mechanics part of this thesis given in Chapter 4.

There are many other formulations for contact mechanics in literature made by Schreppers et al (1992), Taylor et al (1993), Feng (1995), Laursen et al (1997), Chawla et al (1998), Fujun et al (2000), McDevitt et al (2000), Feng et al (2003), Khenous et al (2006), Feng et al (2006), Deufhard et al (2008). Most of them deal with large deformations. Some of them formulates it in 3D and some of them deal with the contact search algorithm, which determines the contact conditions between solids. Most recent studies deal with the contact mechanics consisting of dynamic motions (Deufhard et al 2008), elastodynamic problems (Khenous et al 2006) and some hyperelastic bodies (Feng et al 2003, 2006).

## CHAPTER 2

### FORMULATION OF GEOMETRICALLY NONLINEAR BAR ELEMENT

#### 2.1 General

2D structural truss system is selected as the elastic structure in contact with cable as mentioned in Section 1.2. Therefore, a formulation for bar element having nonlinear geometry is needed. The formulation can be found in various textbooks in the literature, e.g. Bathe (1996). So, a brief summary is given in this chapter.

#### 2.2 Updated Lagrangian Formulation

In Lagrangian incremental analysis approach, the equilibrium of the body at time  $t + \Delta t$  referring to time  $t$  is expressed using the principle of virtual displacements as follows;

$$\int_{^tV} {}^{t+\Delta t}S_{ij} \delta {}^{t+\Delta t}\epsilon_{ij} d^tV = {}^{t+\Delta t}W \quad (2.1)$$

Where  ${}^{t+\Delta t}W$  is the external virtual work,  ${}^{t+\Delta t}S_{ij}$  are the second Piola-Kirchhoff stresses referring to configuration at time  $t$  and  ${}^{t+\Delta t}\epsilon_{ij}$  are the Green-Lagrange strains referring to configuration at time  $t$ .

Knowing that;

$${}^{t+\Delta t}S_{ij} = {}^tS_{ij} + {}^tS_{ij} = {}^t\tau_{ij} + {}^tS_{ij} \quad (2.2)$$

And

$${}^{t+\Delta t}{}_t\mathcal{E}_{ij} = {}_t\mathcal{E}_{ij} \quad (2.3)$$

Where  ${}^t\tau_{ij}$  are the components of the Cauchy stress tensor at time  $t$  and  ${}_t\mathcal{E}_{ij}$  are the components of the Green-Lagrange strain increment tensor in the interval  $(t, t + \Delta t)$  referring to configuration at time  $t$ .

Writing Eq. (2.3) in variational form

$$\delta {}^{t+\Delta t}{}_t\mathcal{E}_{ij} = \delta {}_t\mathcal{E}_{ij} \quad (2.4)$$

Where;

$${}_t\mathcal{E}_{ij} = {}_te_{ij} + {}_t\eta_{ij} \quad (2.5)$$

Where;  ${}_te_{ij}$  is the linear part of  ${}_t\mathcal{E}_{ij}$  with additional initial displacement effect and  ${}_t\eta_{ij}$  is the non-linear part of  ${}_t\mathcal{E}_{ij}$ .

$${}_te_{ij} = \frac{1}{2}({}_tu_{i,j} + {}_tu_{j,i})$$

$${}_t\eta_{ij} = \frac{1}{2}{}_tu_{k,i}{}_tu_{k,j}$$

Substituting Eq. (2.2), Eq. (2.4) and Eq. (2.5) into Eq. (2.1) and using approximations  ${}_tS_{ij} = {}_tC_{ijrs}{}_te_{rs}$  and  $\delta {}_t\mathcal{E}_{ij} = \delta {}_te_{ij}$ , linearized equilibrium equations for Updated Lagrangian formulation is achieved.

$$\int_{{}_tV} {}_tC_{ijrs}{}_te_{rs}\delta {}_te_{ij} dV + \int_{{}_tV} {}^t\tau_{ij}\delta {}_t\eta_{ij} dV = {}^{t+\Delta t}W - \int_{{}_tV} {}^t\tau_{ij}\delta {}_te_{ij} dV \quad (2.6)$$

Substituting the element coordinate and displacement interpolations into Eq. (2.6), governing equation of motion is achieved.

$$({}_t\mathbf{K}_L + {}_t\mathbf{K}_{NL})\Delta\mathbf{U} = {}^{t+\Delta t}\mathbf{F} - {}^t\mathbf{R} \quad (2.7)$$



Where  ${}^t\mathbf{K}_L$  and  ${}^t\mathbf{K}_{NL}$  are the linear and nonlinear part of the structural stiffness matrix,  ${}^{t+\Delta t}\mathbf{F}$  is the vector of applied nodal loads at time  $t + \Delta t$  and  ${}^t\mathbf{R}$  is the vector of equivalent nodal response of equilibrium stresses at time  $t$ . Elements of Eq. (2.7) are defined for truss element in the following part of this chapter.

### 2.2.1 Formulation of Truss Element

The large rotation-small strain finite element formulation for a straight truss element with constant cross-sectional area is considered. The deformations of the element are specified by the displacements of its nodes in the following figure.

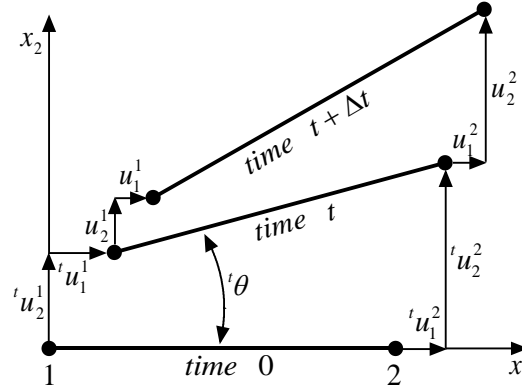


Figure 2.1 Deformation of a bar element

The derivation is simplified by considering a coordinate system aligned with the bar element at time  $t$ .

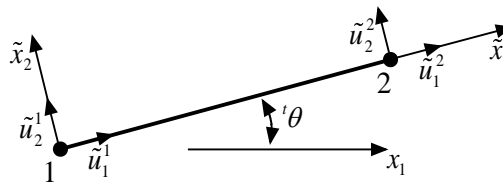


Figure 2.2 Coordinate system of a bar element

Rewriting the principle of virtual work expression defined in Eq. (2.6) in rotated coordinate system and knowing that the only non-zero stress component is  ${}^t\tau_{11}$ ,

$$\int_{{}^tV} {}_t\tilde{C}_{1111} {}_t\tilde{e}_{11} \delta {}_t\tilde{e}_{11} {}^t dV + \int_{{}^tV} {}^t\tilde{\tau}_{11} \delta {}_t\tilde{\eta}_{11} {}^t dV = {}^{t+\Delta t}\tilde{W} - \int_{{}^tV} {}^t\tilde{\tau}_{11} \delta {}_t\tilde{e}_{11} {}^t dV \quad (2.8)$$

Where the tilde on top of a symbol indicates that the parameter is defined in rotated coordinate system.

$${}_t\tilde{C}_{1111} = E$$

$${}^t\tilde{\tau}_{11} = \frac{{}^tP}{A}$$

$${}^tV = AL$$

Hence, Eq. 2.8 becomes

$$(EA) {}_t\tilde{e}_{11} \delta {}_t\tilde{e}_{11} L + {}^tF \delta {}_t\tilde{\eta}_{11} L = {}^{t+\Delta t}\tilde{W} - {}^tF \delta {}_t\tilde{e}_{11} L \quad (2.9)$$

Rewriting Eq. 2.5 for defined coordinate system of bar element,

$${}_t\tilde{e}_{11} = {}_t\tilde{u}_{1,1} \quad (2.10)$$

$${}_t\tilde{\eta}_{11} = \frac{1}{2} \left( ({}_t\tilde{u}_{1,1})^2 + ({}_t\tilde{u}_{2,1})^2 \right) \quad (2.11)$$

In variational form;

$$\delta {}_t\tilde{e}_{11} = \delta {}_t\tilde{u}_{1,1} \quad (2.12)$$

$$\delta {}_t\tilde{\eta}_{11} = \left[ \delta {}_t\tilde{u}_{1,1} \quad \delta {}_t\tilde{u}_{2,1} \right] \begin{bmatrix} {}_t\tilde{u}_{1,1} \\ {}_t\tilde{u}_{2,1} \end{bmatrix} \quad (2.13)$$

Writing Eq. (2.10) and Eq. (2.13) in terms of displacements,

$${}_t\tilde{e}_{11} = {}_t\tilde{u}_{1,1} = \frac{\partial {}_t\tilde{u}_1}{\partial {}^tx_1} = \frac{1}{L} \begin{bmatrix} -1 & 0 & 1 & 0 \end{bmatrix} \tilde{\mathbf{u}} \quad (2.14)$$

$$\delta_{\tau} \tilde{\eta}_{11} = \delta \tilde{\mathbf{u}}^T \left( \frac{1}{L} \begin{bmatrix} -1 & 0 \\ 1 & 0 \\ 0 & 1 \end{bmatrix} \right) \left( \frac{1}{L} \begin{bmatrix} -1 & 0 & 1 & 0 \\ 0 & -1 & 0 & 1 \end{bmatrix} \right) \tilde{\mathbf{u}} \quad (2.15)$$

$$\text{Where } \tilde{\mathbf{u}} = \begin{bmatrix} \tilde{u}_1^1 \\ \tilde{u}_2^1 \\ \tilde{u}_1^2 \\ \tilde{u}_2^2 \end{bmatrix}$$

Substituting Eq. (2.12), Eq. (2.14) and Eq. (2.15) into Eq. (2.9),

$$\begin{aligned} \delta \tilde{\mathbf{u}}^T \left( \frac{EA}{L} \begin{bmatrix} 1 & 0 & -1 & 0 \\ 0 & 0 & 0 & 0 \\ -1 & 0 & 1 & 0 \\ 0 & 0 & 0 & 0 \end{bmatrix} \right) \tilde{\mathbf{u}} + \delta \tilde{\mathbf{u}}^T \left( \frac{{}^tF}{L} \begin{bmatrix} 1 & 0 & -1 & 0 \\ 0 & 1 & 0 & -1 \\ -1 & 0 & 1 & 0 \\ 0 & -1 & 0 & 1 \end{bmatrix} \right) \tilde{\mathbf{u}} \\ = {}^{t+\Delta t}\tilde{W} - \delta \tilde{\mathbf{u}}^T \left( {}^tF \begin{bmatrix} -1 \\ 0 \\ 1 \\ 0 \end{bmatrix} \right) \end{aligned} \quad (2.16)$$

Relation between the local coordinate system and the global coordinate system is given as;

$$\tilde{\mathbf{u}} = \begin{bmatrix} \tilde{u}_1^1 \\ \tilde{u}_2^1 \\ \tilde{u}_1^2 \\ \tilde{u}_2^2 \end{bmatrix} = \begin{bmatrix} \cos {}^t\theta & \sin {}^t\theta & 0 & 0 \\ -\sin {}^t\theta & \cos {}^t\theta & 0 & 0 \\ 0 & 0 & \cos {}^t\theta & \sin {}^t\theta \\ 0 & 0 & -\sin {}^t\theta & \cos {}^t\theta \end{bmatrix} \begin{bmatrix} u_1^1 \\ u_2^1 \\ u_1^2 \\ u_2^2 \end{bmatrix} \quad (2.17)$$

Substituting Eq. (2.17) into Eq. (2.16), linear and nonlinear parts of the stiffness matrix and the internal response vector of the equation of motion defined in global coordinate system are obtained.

$${}^t\mathbf{K}_L = \frac{EA}{L} \begin{bmatrix} (\cos {}^t\theta)^2 & (\cos {}^t\theta)(\sin {}^t\theta) & -(\cos {}^t\theta)^2 & -(\cos {}^t\theta)(\sin {}^t\theta) \\ & (\sin {}^t\theta)^2 & -(\cos {}^t\theta)(\sin {}^t\theta) & -(\sin {}^t\theta)^2 \\ & \text{sym} & (\cos {}^t\theta)^2 & (\cos {}^t\theta)(\sin {}^t\theta) \\ & & & (\sin {}^t\theta)^2 \end{bmatrix} \quad (2.18)$$

$${}^t\mathbf{K}_{NL} = \frac{{}^tF}{L} \begin{bmatrix} 1 & 0 & -1 & 0 \\ 0 & 1 & 0 & -1 \\ -1 & 0 & 1 & 0 \\ 0 & -1 & 0 & 1 \end{bmatrix} \quad (2.19)$$

$${}^t\mathbf{R} = {}^tF \begin{bmatrix} -\cos {}^t\theta \\ -\sin {}^t\theta \\ \cos {}^t\theta \\ \sin {}^t\theta \end{bmatrix} \quad (2.20)$$

Hence, deformations of a bar element is obtained by applying Eq. (2.18), Eq. (2.19) and Eq. (2.20) in Eq. (2.7). Correct result for deformations are reached through Newton-Raphson iterations, which is a well-known procedure for the solution of nonlinear equations.

## CHAPTER 3

### SINGLE AND MULTI-SEGMENT CABLE

#### 3.1 Single-Segment Cable Analysis

Cables display nonlinear behavior under transverse loading. In the past, this behavior was undervalued or some simplifying assumptions were made. The Method of Imaginary Reactions was proposed by Skop and O'Hara (1970) and improved by Polat (1981) to handle with this nonlinearity and/or to solve cable correctly. In this method, cable is defined as a determinant structural system by assigning a reaction to one of its ends. This reaction determines the position of the other end. Therefore, there is a relation between the assumed reaction at one end and the position of the second end. This relation is defined as a stiffness matrix of cable. Solution of cable is achieved iteratively by using stiffness matrix. Formulation of stiffness matrix of cable and iterative procedures are defined below.

##### 3.1.1 Cable Equilibrium Equations

A cable, having total unstressed length  $L_u$  and stressed length  $L_s$ , is supported between points  $A$  and  $B$ . Cable in space is shown in Figure 3.1.

As in Figure 3.1,  $\vec{P}_A$  and  $\vec{P}_B$  are the position vectors of supports at the ends of the cable. Let  $M$  be any point on the cable defined by the following parameters;

$l_u$  ; unstressed arc length form point  $A$  to  $M$  .

$l_s$  ; stressed arc length from point  $A$  to  $M$  .

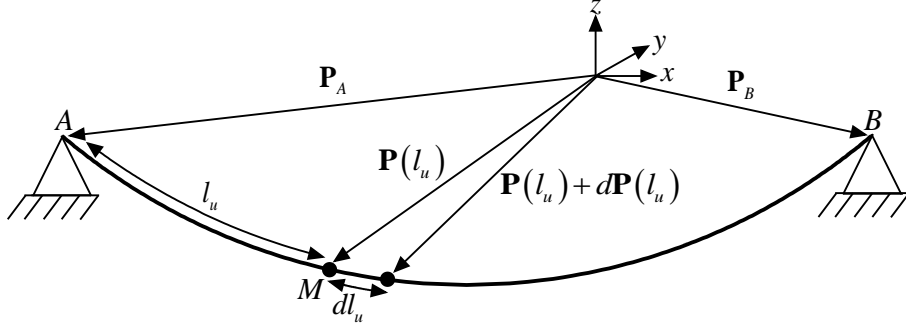


Figure 3.1 Configuration of single-segment cable in space.

Relation between  $d\mathbf{P}(l_u)$  and  $dl_s$  is defined with the unit tangent along the cable,  $\hat{\mathbf{t}}(l_u)$ .

$$d\mathbf{P}(l_u) = -\hat{\mathbf{t}}(l_u)dl_s \quad (3.1)$$

The unknowns in Eq. (3.1) are;  $\hat{\mathbf{t}}(l_u)$  and the differential stressed arc length of the cable  $dl_s$ .

The unit tangent along the cable can also be defined with  $\mathbf{R}(l_u)$  and  $T(l_u)$  which are reaction vector at  $l_u$  and tension at  $l_u$ , respectively.

$$\hat{\mathbf{t}}(l_u) = \frac{\mathbf{R}(l_u)}{T(l_u)} \quad (3.2)$$

The elongation of the differential element is;

$$\Delta l_u = dl_s - dl_u \quad (3.3)$$

The strain of this element is the elongation divided by the original length.

$$\varepsilon(l_u) = \frac{dl_s - dl_u}{dl_u} \quad (3.4)$$

From Eq. (3.4) the stressed length of the element can be written as;

$$dl_s = [1 + \varepsilon(l_u)] dl_u \quad (3.5)$$

Substituting Eq. (3.5) into Eq. (3.1),

$$\frac{d\mathbf{P}(l_u)}{dl_u} = -\hat{\mathbf{t}}(l_u)[1 + \varepsilon(l_u)] \quad (3.6)$$

Finally, writing Eq. (3.6) in integral form,

$$\mathbf{P}(l_u) = \mathbf{P}(0) - \int_0^{l_u} \frac{\mathbf{R}(x)}{T(x)} [1 + \varepsilon(l_u)] dx \quad (3.7a)$$

Since  $\mathbf{P}(0) = \mathbf{P}_A$ ,

$$\mathbf{P}(l_u) = \mathbf{P}_A - \int_0^{l_u} \frac{\mathbf{R}(x)}{T(x)} [1 + \varepsilon(l_u)] dx \quad (3.7b)$$

Consequently,  $\mathbf{R}_A$ , which is equal to  $\mathbf{R}(l_0)$ , is the only unknown in this equation and it can be regarded as the initial condition of the problem.

### 3.1.2 Stiffness Matrix

If a virtual displacement,  $\Delta\mathbf{P}_B$ , is given to support  $B$ , there will be a change in the reactions at the other support,  $\Delta\mathbf{R}_A$ . The relation between these parameters are explained by the stiffness matrix,  $\mathbf{K}$ .

$$\Delta\mathbf{R}_A = \mathbf{K}\Delta\mathbf{P}_B \quad (3.8)$$

The stiffness matrix is determined by using the variational approach as follows:

From variation of Eq. 3.7b,  $\Delta\mathbf{P}_B$  is determined.

$$\begin{aligned}
\Delta \mathbf{P}_B &= - \int_0^{L_u} \Delta \left\{ \left[ 1 + \varepsilon(l_u) \right] \frac{\mathbf{R}(l_u)}{T(l_u)} \right\} dl_u \\
&= - \int_0^{L_u} \left\{ \frac{1 + \varepsilon(l_u)}{T(l_u)} \Delta \mathbf{R}(l_u) + \mathbf{R}(l_u) \Delta \left( \frac{1 + \varepsilon(l_u)}{T(l_u)} \right) \right\} dl_u
\end{aligned} \tag{3.9}$$

Unknowns are  $T(l_u)$ ,  $\Delta \mathbf{R}(l_u)$  and  $\Delta \left( \frac{1 + \varepsilon(l_u)}{T(l_u)} \right)$  in Eq. (3.9).

$$\begin{aligned}
\Delta \left( \frac{1 + \varepsilon(l_u)}{T(l_u)} \right) &= \frac{\Delta [1 + \varepsilon(l_u)] T(l_u) - [1 + \varepsilon(l_u)] \Delta T(l_u)}{T^2(l_u)} \\
&= \frac{\Delta \varepsilon(l_u) T(l_u) - [1 + \varepsilon(l_u)] \Delta T(l_u)}{T^2(l_u)}
\end{aligned} \tag{3.10}$$

Thus, unknowns are  $T(l_u)$ ,  $\Delta T(l_u)$ ,  $\Delta \mathbf{R}(l_u)$ ,  $\Delta \varepsilon(l_u)$  in Eq. (3.9).

Tension in cable is;

$$T(l_u) = [\mathbf{R}(l_u) \cdot \mathbf{R}(l_u)]^{1/2} \tag{3.11}$$

In variational form;

$$\Delta T(l_u) = \frac{1}{2} \frac{[\mathbf{R}(l_u) \cdot \Delta \mathbf{R}(l_u) + \Delta \mathbf{R}(l_u)]}{[\mathbf{R}(l_u) \cdot \mathbf{R}(l_u)]^{1/2}} \tag{3.12}$$

Or

$$\Delta T(l_u) = \frac{\mathbf{R}(l_u) \cdot \Delta \mathbf{R}(l_u)}{T(l_u)} \tag{3.13}$$



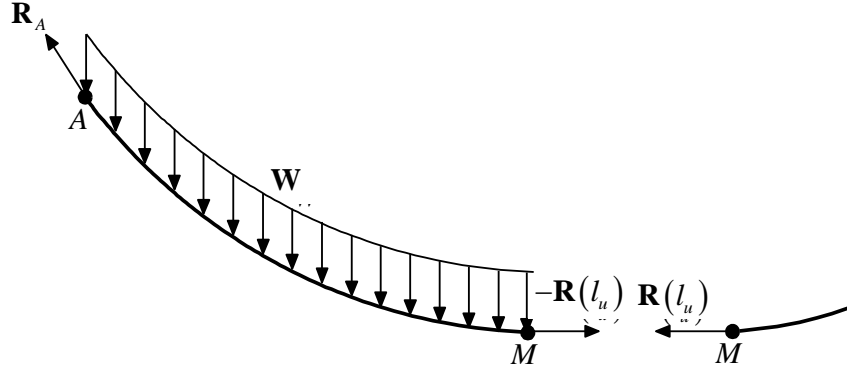


Figure 3.2 Reactions on cable

Many external forces, could be applied to the cable. If no external load is applied, there will be only self-weight of the cable.

$$\mathbf{F}_{ext}(l_u) = \mathbf{W}l_u \quad (3.14)$$

From the free body diagram of cable element shown in Figure 3.2, reaction at point  $M$  is;

$$\mathbf{R}(l_u) = \mathbf{R}_A + \mathbf{F}_{ext}(l_u) \quad (3.15a)$$

For the whole cable

$$\mathbf{R}(L_U) = \mathbf{R}_A + \mathbf{F}_{ext}(L_U) \quad (3.15b)$$

$$\mathbf{R}_B = \mathbf{R}(L_U) \quad (3.16)$$

Substituting Eq. (3.16) into Eq. (3.15b),

$$\mathbf{R}_B = \mathbf{R}_A + \mathbf{F}_{ext}(L_U) \quad (3.17)$$

From variation of Eq. (3.17),

$$\Delta \mathbf{R}(l_u) = \Delta \mathbf{R}_A = \Delta \mathbf{R}_B \quad (3.18)$$

The strain can also be expressed by the stress-strain relationship as;

$$\varepsilon(l_u) = \frac{T(l_u)}{EA} \nu \quad (3.19)$$

$T(l_u)$  is the tension at  $M$  and  $E$ ,  $A$  and  $\nu$  are material properties of cable.

The variational form of strain,  $\Delta\varepsilon(l_u)$ , from Eq. (3.4).

$$\Delta\varepsilon(l_u) = \nu \left[ \frac{T(l_u)}{EA} \right]^{\nu-1} \frac{\Delta T(l_u)}{EA} \quad (3.20a)$$

$$= \nu \varepsilon(l_u) \frac{\mathbf{R}(l_u) \cdot \Delta \mathbf{R}(l_u)}{T^2(l_u)} \quad (3.20b)$$

So, substituting Eq. (3.11) Eq. (3.13) and Eq. (3.20b) into Eq. (3.10),

$$\begin{aligned} \Delta \left[ \frac{1 + \varepsilon(l_u)}{T(l_u)} \right] &= \frac{\nu \varepsilon(l_u) \frac{\mathbf{R}(l_u) \cdot \Delta \mathbf{R}(l_u)}{T^2(l_u)} T(l_u) - [1 + \varepsilon(l_u)] \frac{\mathbf{R}(l_u) \cdot \Delta \mathbf{R}(l_u)}{T(l_u)}}{T^2(l_u)} \\ &= - \frac{1 + (1 - \nu) \varepsilon(l_u)}{T^3(l_u)} [\mathbf{R}(l_u) \cdot \Delta \mathbf{R}(l_u)] \end{aligned} \quad (3.21)$$

Finally, substituting Eq. (3.18) and Eq. (3.21) into Eq. (3.9),

$$\Delta \mathbf{P}_B = - \int_0^{L_U} \left\{ \left| \frac{1 + \varepsilon(l_u)}{T(l_u)} \right| \Delta \mathbf{R}_A - \left| \frac{1 + (1 - \nu) \varepsilon(l_u)}{T^3(l_u)} \right| [\mathbf{R}(l_u) \cdot \Delta \mathbf{R}_A] \mathbf{R}(l_u) \right\} dl_u \quad (3.22)$$

In global coordinate directions Eq. (3.22) will be;

$$\Delta P_{BX} \hat{\mathbf{i}} = - \int_0^{L_U} \left[ C_1 \Delta R_{AX} \hat{\mathbf{i}} - C_2 C_3 C_4 \right] dl_u \quad (3.23a)$$

$$\Delta P_{BY} \hat{\mathbf{j}} = - \int_0^{L_U} \left[ C_1 \Delta R_{AY} \hat{\mathbf{j}} - C_2 C_3 C_4 \right] dl_u \quad (3.23b)$$

$$\Delta P_{BZ} \hat{\mathbf{k}} = - \int_0^{L_U} \left[ C_1 \Delta R_{AZ} \hat{\mathbf{k}} - C_2 C_3 C_4 \right] dl_u \quad (3.23c)$$

Where;

$$C_1 = \left[ \frac{1 + \varepsilon(l_u)}{T(l_u)} \right]$$

$$C_2 = \left[ \frac{1 + (1 - \nu)\varepsilon(l_u)}{T^3(l_u)} \right]$$

$$C_3 = [R_X(l_u)\Delta R_{AX} + R_Y(l_u)\Delta R_{AY} + R_Z(l_u)\Delta R_{AZ}]$$

$$C_4 = [R_X(l_u)\hat{\mathbf{i}} + R_Y(l_u)\hat{\mathbf{j}} + R_Z(l_u)\hat{\mathbf{k}}]$$

Writing Eq. (3.23a, b, c) in the form of Eq. (3.8).

$$\begin{Bmatrix} \Delta P_{BX} \\ \Delta P_{BY} \\ \Delta P_{BZ} \end{Bmatrix} = \mathbf{K}^{-1} \begin{Bmatrix} \Delta R_{AX} \\ \Delta R_{AY} \\ \Delta R_{AZ} \end{Bmatrix} \quad (3.24)$$

Where the stiffness matrix is;

$$\mathbf{K} = \begin{bmatrix} -\int_0^{L_e} [C_1 - C_2 R_X^2(l_u)] dl_u & -\int_0^{L_e} [C_2 R_X(l_u) R_Y(l_u)] dl_u & -\int_0^{L_e} [C_2 R_X(l_u) R_Z(l_u)] dl_u \\ -\int_0^{L_e} [C_2 R_Y(l_u) R_X(l_u)] dl_u & -\int_0^{L_e} [C_1 - C_2 R_Y^2(l_u)] dl_u & -\int_0^{L_e} [C_2 R_Y(l_u) R_Z(l_u)] dl_u \\ -\int_0^{L_e} [C_2 R_Z(l_u) R_X(l_u)] dl_u & -\int_0^{L_e} [C_2 R_Z(l_u) R_Y(l_u)] dl_u & -\int_0^{L_e} [C_1 - C_2 R_Z^2(l_u)] dl_u \end{bmatrix}$$

Inverse of stiffness matrix is the flexibility matrix,  $\mathbf{F} = \mathbf{K}^{-1}$ .

So, Eq. (3.8) can be rewritten as;

$$\Delta P_B = \mathbf{K}^{-1} \Delta R_A \quad (3.25a)$$

or

$$\Delta P_B = \mathbf{F} \Delta R_A \quad (3.25b)$$

### 3.1.3 Newton-Raphson Method

Being an iterative technique, Newton-Raphson method is used to solve equations numerically. The method is based on making linear approximations to achieve a solution for nonlinear systems. Aim is to reach the solution linearly. Therefore, solutions are always approximate. It is appropriate to find a solution for nonlinear behavior of cable by Newton-Raphson Method.

It is seen in Eq. (3.7b) that the position of cable is a function of  $\mathbf{R}_A$ . However, it is not known for equilibrium state  $\mathbf{R}_{A,sol}$ . Newton-Raphson method is used to find a solution with linear approximations.

The step-by-step procedure to find the unknown support reactions of cable is explained below and described schematically in Figure 3.3.

1. Initiate the solution by defining a reaction  $\mathbf{R}_A^{[i]}$ .
2. Determine the cable configuration, position of the cable end  $\mathbf{P}^{[i]}(L_U)$  and stiffness matrix  $\mathbf{K}^{[i]}$ .
3. Determine the misclose vector and the error as;

$$\mathbf{M}^{[i]} = \mathbf{P}_B - \mathbf{P}^{[i]}(L_U) \quad (3.26)$$

$$E^{[i]} = |\mathbf{M}^{[i]}| \quad (3.27)$$

4. Calculate a better approximation for  $\mathbf{R}_A^{[i]}$ .

$$\mathbf{R}_A^{[i+1]} = \mathbf{R}_A^{[i]} + (\mathbf{K}^{[i]})^{-1} \mathbf{M}^{[i]} \quad (3.28)$$

5. Go to step 2 and continue iterations until  $E^{[i]} \leq ERR$ . where  $ERR$  is the target error for approximate result.

Assigning an initial reaction for the support is a very important step for the solution. A better assign will decrease the amount of iteration very much.

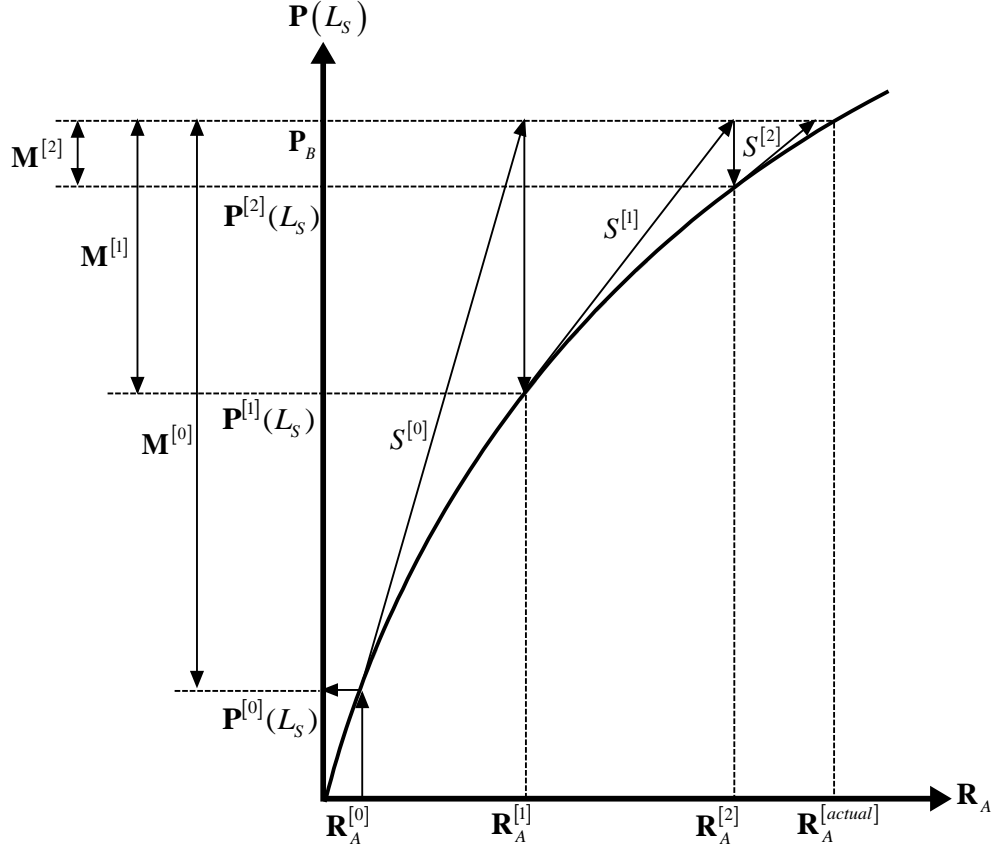


Figure 3.3 Newton-Raphson method in schematic form for single-segment cable

### 3.2 Multi-Segment Cable Analysis

Multi-segment cables are monolithic cables with multiple intermediate supports. Cable is free to slide on supports by defined stationary and frictionless intermediate roller supports. Method was proposed by Demir (2011). In that research, cable is divided into a number of elements and each segment is analyzed as an independent single-segment cable. The stress continuity requirement between the adjacent cable segments is enforced in each iteration until complete equilibrium is reached. Two analysis methods were proposed in research of Demir (2011): Direct stiffness approach and tension distribution method.

### 3.2.1 Direct Stiffness Approach

The only unknown for defined system is the length of each segment. So, total cable length is distributed to each segment to start the solution procedure. Unstressed length of  $i^{th}$  segment is denoted by  $l_{u(i)}$  as seen in Figure 3.4.

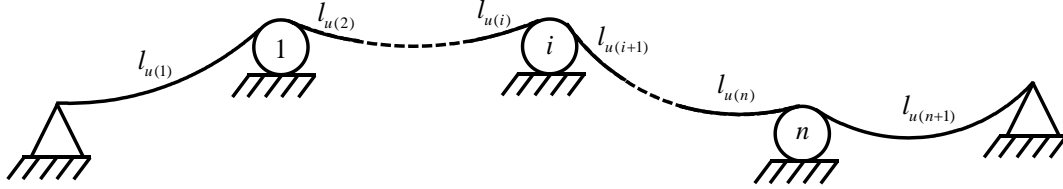


Figure 3.4 Configuration of multi-segment continuous cable

Thus, total unstressed length of the system having  $n$  segment is;

$$L_U = \sum_{i=1}^n l_{u(i)} \quad (3.29)$$

Each segment is solved by single-segment cable procedure by knowing its cable length. Thus, tensions at the cusp of segments are known for each single segment cable solution. Wrong distribution of segmental lengths will lead to unbalanced tension of cable on roller supports. This unbalanced tension at  $i^{th}$  roller support ( $i^{th}$  roller support is the connection point of  $i^{th}$  segment and  $(i+1)^{th}$  segment) is given in Eq. (3.30) as  $\Delta T_{(i)}$ .

$$\Delta T_{(i)} = \left| \vec{R}_{F(i+1)} \right| - \left| \vec{R}_{L(i)} \right| \quad (3.30)$$

Where  $\vec{R}_{F(i+1)}$  and  $\vec{R}_{L(i)}$  are shown in Figure 3.5.

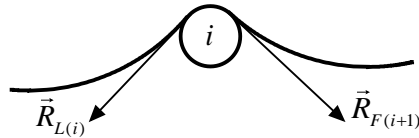


Figure 3.5 Cable tensions at support  $i$ .

There must be some unstressed length adjustments  $\{\Delta L_U\}$  between neighboring segments, which makes cable system into complete equilibrium.

$$\Delta L_{U(i)}^{segment} = -\Delta L_{U(i)} \quad (3.31a)$$

$$\Delta L_{U(i+1)}^{segment} = \Delta L_{U(i)} \quad (3.31b)$$

Where;  $\Delta L_{U(i)}^{segment}$  and  $\Delta L_{U(i+1)}^{segment}$  are the changes in unstressed length of segments  $i$  and  $i+1$ , respectively, and  $\Delta L_{U(i)}$  is the adjustment applied to cable segments at support  $i$ .

In the course of iterative solution process for the equilibrium state of cable system, there is always a need for some correction in the currently assumed distribution of total cable length among its segments. This is necessary to move closer to the equilibrium state by minimizing the unbalanced reactions between cable segments. It can be achieved, if a quasi-linear behavior of the system is assumed at the end of each predictive solution step. With this assumption, we can set up a relationship between the anticipated unstressed length adjustment  $\delta L_{U(j)}$  at any support  $j$  and the corresponding change it would create in the unbalanced reactions at support  $i$ . This change in unbalanced reactions,  $\delta T_{(i)}$  can be expressed as follows.

$$\delta T_{(i)} = K_{ij} \cdot \delta L_{U(j)} \quad (3.32a)$$

Or in matrix form;

$$\{\delta T\} = [K] \cdot \{\delta L_U\} \quad (3.32b)$$

Where;

$$\{\delta T\} = \begin{Bmatrix} \delta T_{(1)} \\ \delta T_{(2)} \\ \vdots \\ \delta T_{(n)} \end{Bmatrix}$$

$$\{\delta L_U\} = \begin{Bmatrix} \delta L_{U(1)} \\ \delta L_{U(2)} \\ \vdots \\ \delta L_{U(n)} \end{Bmatrix}$$

$$K = \begin{bmatrix} K_{11} & \cdots & K_{1n} \\ \vdots & \ddots & \vdots \\ K_{n1} & \cdots & K_{nn} \end{bmatrix}$$

Coefficient matrix  $[K]$  can be regarded as a stiffness matrix with each term  $K_{ij}$  giving the change in unbalanced reactions  $\delta T_{(i)}$  at support  $i$  due to a change in unstressed length  $\delta L_{U(j)}$  at support  $j$  between cable segments  $j$  and  $j+1$ .

The tangential stiffness matrix  $[K]$  in Eq. (3.33) can be constructed column-by-column by adjusting the unstressed lengths of cable segments at support  $j$  by a small amount  $\delta l$  and calculating the resulting changes in the unbalanced reactions  $\delta t_{(i)}$  at all support locations from the reanalysis of the cable system with the changed segment lengths at support  $j$ . The  $j^{th}$  column of  $[K]$  is then obtained as;

$$K_i = \delta t_{(i)} / \delta l \quad (i = 1, 2, \dots, n) \quad (3.33)$$

In the correction step, the objective is to find the required amount of length adjustment at each support to eliminate the current values of unbalanced reactions at supports. This is obtained from Eq. (3.32b) as;

$$\{\Delta L_U\} = [K]^{-1} \cdot \{\Delta T\} = [F] \cdot \{\Delta T\} \quad (3.34)$$

Where the matrix  $[F]$  can be regarded as a kind of flexibility matrix giving the changes in cable segment lengths for a set of axial forces applied along the cable at internal supports (segment junctions). If the cable behavior were linear as assumed, the length adjustments  $\{\Delta L_U\}$  of Eq. (3.34) would eliminate the unbalanced reactions at internal supports and bring the cable system into true equilibrium.



However, in general, this will not be the case since the cable behavior is nonlinear and some additional iterations will be needed before reaching the final equilibrium. Therefore, Newton-Raphson iterations are continued in this predictive/corrective algorithm to reach the final equilibrium state.

Length adjustments for whole system can be applied by Eq. (3.35) for Newton-Raphson iteration number  $m + 1$ .

$$l_{u(i)}^{[m+1]} = l_{u(i)}^{[m]} + \delta L_{U(i)}^{segment} \quad (3.35)$$

### 3.2.2 Tension Distribution Method (Relaxation Method)

Tension distribution method is adapted from the moment distribution method, which is commonly used for the analysis of continuous beams. This method is a special form of the direct stiffness approach. The basic difference is in the way the cable segment lengths are adjusted for a better approximation to equilibrium state. In Direct stiffness approach, the increment for each segment is determined for whole system by calculating the stiffness matrix of the system totally. On the other hand, in tension distribution method, increment of two adjacent segments are determined by calculating the stiffness matrix of connecting roller support while keeping all other segment lengths as they are. Therefore, in the corrective stage following a predictive solution, an influence (stiffness) coefficient is calculated at a selected joint first by introducing a virtual adjustment at the joint and the actual amount of adjustment required to eliminate the unbalanced reaction at the joint is determined based on this information. A cycle will be completed for whole system, if increment on each roller support is found and applied. So, iterative cyclic calculations are carried out until an equilibrium state is reached where the unbalanced reactions at internal supports became negligibly small.

It is expected that; application of length adjustment  $\Delta L_{U(i)}$ , for  $i^{th}$  roller support make the tension difference  $\Delta T_{(i)}$ , zero. Relation between  $\Delta L_{U(i)}$  and  $\Delta T_{(i)}$  is expressed in Eq. (3.36).

$$\Delta T_{(i)} = k_{(i)} \cdot \Delta L_{U(i)} \quad (3.36)$$

The tangential stiffness matrix of  $i^{th}$  roller support  $k_{(i)}$ , can be found by adjusting the unstressed lengths of adjacent segments by a small amount  $\delta l$  and calculating the resulting changes in the unbalanced reactions  $\delta t$  at that support.

$$k_{(i)} = \delta t / \delta l \quad (3.37)$$

Length adjustment for that roller support can be found with Eq. (3.38),

$$\delta L_{U(i)} = k_{(i)}^{-1} \cdot \delta T_{(i)} = f \cdot \delta T_{(i)} \quad (3.38)$$

As was mentioned, it is expected that; unbalanced tension on each roller support be zero in one cycle of length adjustments. However, it is not possible due to nonlinear behavior of cable. Therefore, Newton-Raphson iterations are used to handle with that nonlinearity.

Length adjustments for adjacent segments can be applied by Eq. 3.35 for Newton-Raphson iteration number  $m+1$ .

## CHAPTER 4

### CONTACT MECHANICS

#### 4.1 General

Contact mechanics have been in use for the solution of solids in contact. There is extensive research on the topic. Problem is very complex and computationally difficult. Complexity is due to the combination of different solids. Computational difficulty is due to searches for contact occurrence. Basically, two structures in space have their own solutions. If they are in interaction or in contact, solution will be integrated. These integrated calculations are called contact mechanics.

A contact is basically composed of interaction of two or more structures. Considering the contact between two structures, one of them is termed as target and the other as contactor. Both have their own domain in space. Invasion of their domains is called as contact occurrence. This invasion can be eliminated by applying corresponding contact forces. Potential of a contact due to invasion will be defined in this chapter.

As far as the mechanical behavior is concerned, a contact can be classified into two: Sticking and sliding contact. In sticking contact of discretized structures, there is no relative motion between the contact node and the target surface. In contrast, there is a change in position between the contact node and the target body in sliding contact. Potentials of sticking and sliding conditions are different from each other.

A simple contact having one target element and one contact node is defined geometrically, before defining the potentials of sticking and sliding conditions. Nodes of target element are denoted as A and B. Contact node is denoted as k. Contact point is denoted as C and some vector definitions are given as follows:

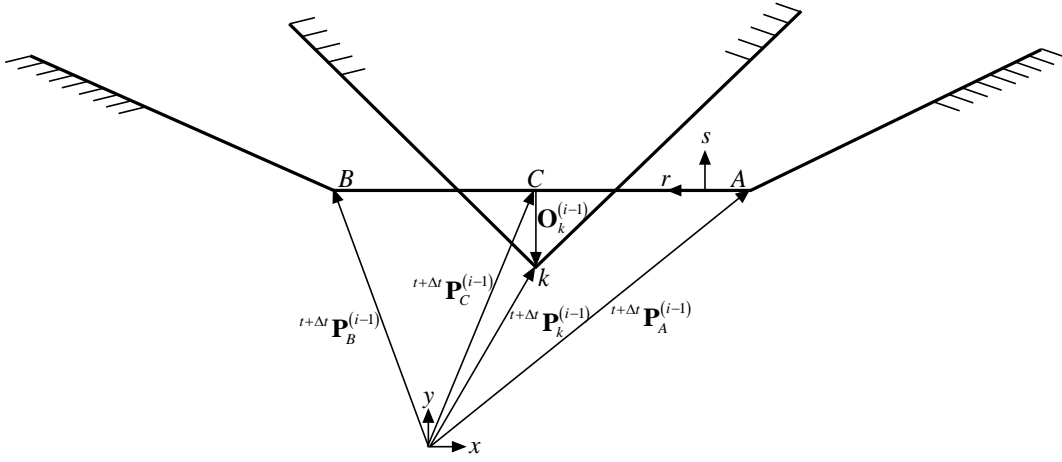


Figure 4.1 Geometry of contact

${}^{t+\Delta t}\mathbf{P}_A^{(i-1)}$  = Position vector for node A after iteration  $(i-1)$  at time  $(t + \Delta t)$

${}^{t+\Delta t}\mathbf{P}_B^{(i-1)}$  = Position vector for node B after iteration  $(i-1)$  at time  $(t + \Delta t)$

${}^{t+\Delta t}\mathbf{P}_k^{(i-1)}$  = Position vector for node k after iteration  $(i-1)$  at time  $(t + \Delta t)$

${}^{t+\Delta t}\mathbf{P}_C^{(i-1)}$  = Position vector for point C after iteration  $(i-1)$  at time  $(t + \Delta t)$

$\mathbf{O}_k^{(i-1)}$  = Overlap

$d_j^{(i-1)}$  = Length of the segment.

$\mathbf{n}_r, \mathbf{n}_s$  = Unit vectors along local axes r, s

$\mathbf{i}, \mathbf{j}$  = Unit vectors along global axes x, y

$\beta^{(i-1)}$  = A parameter about the location of C

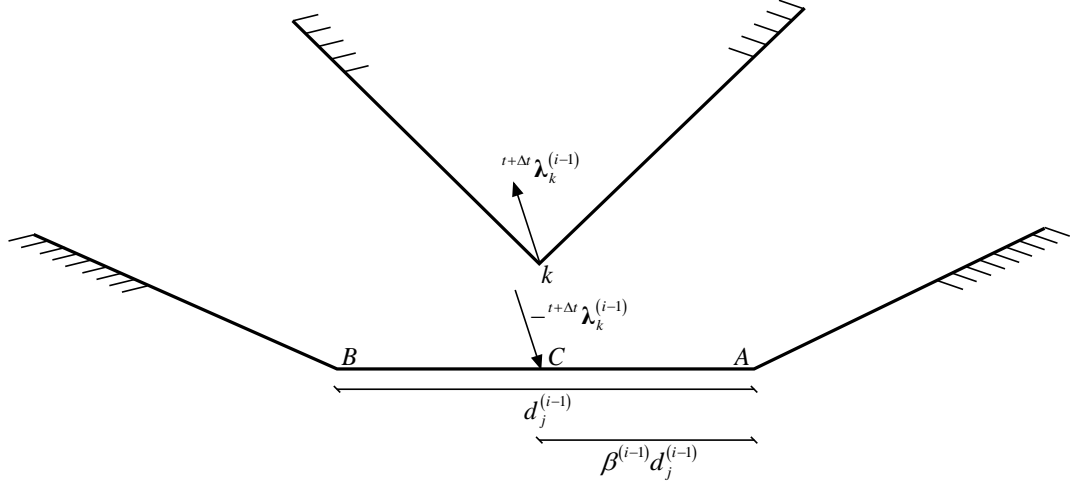


Figure 4.2 Contact forces

${}^{t+\Delta t}\lambda_k^{(i-1)}$  = Contact force at node k

## 4.2 Potential of Sticking Contact

A contact is classified as sticking contact if it satisfies either of following two conditions. First, point k has penetrated into the target body in  $(i-1)^{th}$  iteration whereas there is no contact in  $(i-2)^{th}$  iteration. Second, point k has penetrated into the target surface at  $(i-1)^{th}$  iteration and exerted a force on target surface (traction force), which is smaller than frictional capacity.

In sticking contact, it is assumed that the force applied to the target surface cause sticking which means that relative motion between contact and target is zero. In other words, position of point C with respect to node A and B does not change after the iteration. This leads to an assumption that;  $\beta^{(i-1)}$  does not change during sticking condition. Accordingly, potential of contact forces for sticking contact is derived below.

Overlap can be written as;

$$\mathbf{O}_k^{(i-1)} = {}^{t+\Delta t}\mathbf{P}_k^{(i-1)} - {}^{t+\Delta t}\mathbf{P}_C^{(i-1)} \quad (4.1)$$

Length of the element is;

$$d_j^{(i-1)} = \mathbf{n}_r^T \left[ {}^{t+\Delta t} \mathbf{P}_B^{(i-1)} - {}^{t+\Delta t} \mathbf{P}_A^{(i-1)} \right] \quad (4.2)$$

Corresponding  $\beta^{(i-1)}$  is;

$$\beta^{(i-1)} = \frac{\mathbf{n}_r^T}{d_j^{(i-1)}} \left[ {}^{t+\Delta t} \mathbf{P}_C^{(i-1)} - {}^{t+\Delta t} \mathbf{P}_A^{(i-1)} \right] = \frac{\mathbf{n}_r^T}{d_j^{(i-1)}} \left[ \left( {}^{t+\Delta t} \mathbf{P}_k^{(i-1)} - \mathbf{O}_k^{(i-1)} \right) - {}^{t+\Delta t} \mathbf{P}_A^{(i-1)} \right] \quad (4.3)$$

Reactional forces at node A and B can be written in terms of the contact force and

$\beta^{(i-1)}$ ;

$${}^{t+\Delta t} \boldsymbol{\lambda}_A^{(i-1)} = - \left( 1 - \beta^{(i-1)} \right) {}^{t+\Delta t} \boldsymbol{\lambda}_k^{(i-1)} \quad (4.4a)$$

$${}^{t+\Delta t} \boldsymbol{\lambda}_B^{(i-1)} = - \beta^{(i-1)} {}^{t+\Delta t} \boldsymbol{\lambda}_k^{(i-1)} \quad (4.4b)$$

Corresponding potential is;

$$\omega_k = {}^{t+\Delta t} \boldsymbol{\lambda}_k^{(i)T} \left( \Delta \mathbf{u}_k^{(i)} + \mathbf{O}_k^{(i-1)} \right) + {}^{t+\Delta t} \boldsymbol{\lambda}_A^{(i)T} \Delta \mathbf{u}_A^{(i)} + {}^{t+\Delta t} \boldsymbol{\lambda}_B^{(i)T} \Delta \mathbf{u}_B^{(i)} \quad (4.5)$$

Where;  $\Delta \mathbf{u}_A^{(i)}$ ,  $\Delta \mathbf{u}_B^{(i)}$ ,  $\Delta \mathbf{u}_k^{(i)}$  are incremental displacements at nodes A, B and k in  $(i)^{th}$  iteration, respectively.

Assuming that  $\beta$  does not change during sticking contact condition (as explained before), potential can be written in terms of  $\beta^{(i-1)}$ .

$$\omega_k = {}^{t+\Delta t} \boldsymbol{\lambda}_k^{(i)T} \left( \Delta \mathbf{u}_k^{(i)} + \mathbf{O}_k^{(i-1)} \right) + \left( - \left( 1 - \beta^{(i-1)} \right) {}^{t+\Delta t} \boldsymbol{\lambda}_k^{(i)} \right)^T \Delta \mathbf{u}_A^{(i)} + \left( - \beta^{(i-1)} {}^{t+\Delta t} \boldsymbol{\lambda}_k^{(i)} \right)^T \Delta \mathbf{u}_B^{(i)}$$

Or

$$\omega_k = {}^{t+\Delta t} \boldsymbol{\lambda}_k^{(i)T} \left[ \left( \Delta \mathbf{u}_k^{(i)} + \mathbf{O}_k^{(i-1)} \right) - \left( 1 - \beta^{(i-1)} \right) \Delta \mathbf{u}_A^{(i)} - \beta^{(i-1)} \Delta \mathbf{u}_B^{(i)} \right] \quad (4.6)$$

New contact force at node k is defined in terms of old contact force and change in contact force, as follows.

$${}^{t+\Delta t}\boldsymbol{\lambda}_k^{(i)} = {}^{t+\Delta t}\boldsymbol{\lambda}_k^{(i-1)} + \Delta\boldsymbol{\lambda}_k^{(i)} \quad (4.7)$$

Substituting Eq. (4.7) into Eq. (4.6),

$$\omega_k = \left( {}^{t+\Delta t}\boldsymbol{\lambda}_k^{(i-1)} + \Delta\boldsymbol{\lambda}_k^{(i)} \right)^T \left[ \left( \Delta\mathbf{u}_k^{(i)} + \mathbf{O}_k^{(i-1)} \right) - \left( 1 - \beta^{(i-1)} \right) \Delta\mathbf{u}_A^{(i)} - \beta^{(i-1)} \Delta\mathbf{u}_B^{(i)} \right] \quad (4.8)$$

Displacement of point C can be written as;

$$\Delta\mathbf{u}_C^{(i)} = \left[ \left( 1 - \beta^{(i-1)} \right) \Delta\mathbf{u}_A^{(i)} + \beta^{(i-1)} \Delta\mathbf{u}_B^{(i)} \right] \quad (4.9)$$

Potential is redefined by substituting Eq. (4.9) into Eq. (4.8);

$$\omega_k = \left( {}^{t+\Delta t}\boldsymbol{\lambda}_k^{(i-1)} + \Delta\boldsymbol{\lambda}_k^{(i)} \right)^T \left[ \Delta\mathbf{u}_k^{(i)} + \mathbf{O}_k^{(i-1)} - \Delta\mathbf{u}_C^{(i)} \right] \quad (4.10)$$

Derived potential can be perceived from figure below.

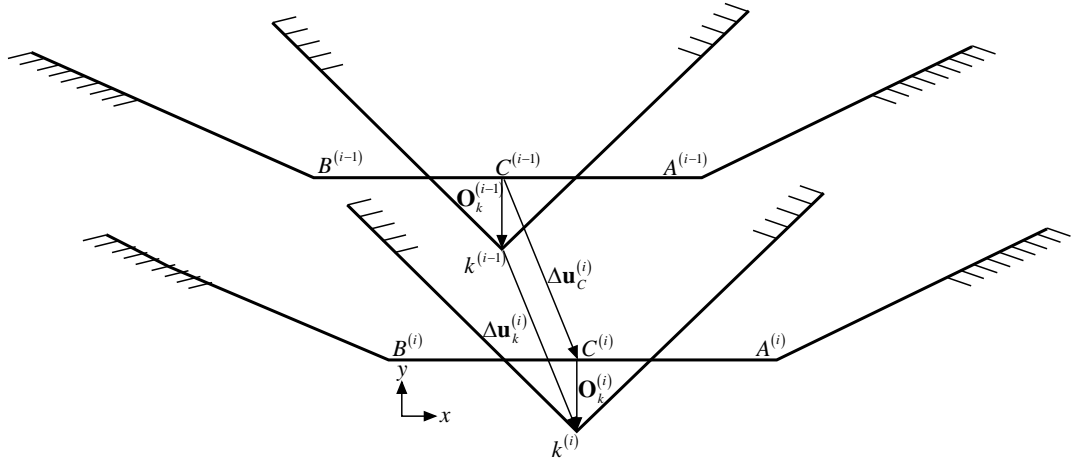


Figure 4.3 Geometry of contact in sticking condition

### 4.3 Potential of Sliding Contact

A contact is classified as sliding contact if it satisfies following condition: Point  $k$  has penetrated into the target surface at  $(i-1)^{th}$  iteration and exerted a force on target surface (traction force), which is greater than frictional capacity.

In sliding contact, contact node applies a force on target element, which has traction force greater than frictional capacity. Therefore, projection point of contact node  $k$  on target element, which is named as  $C$ , changes its position. This means that  $\beta$  changes during iteration. However, frictional force is assumed to be constant during iteration. So potential becomes;

$$\omega_k = {}^{t+\Delta t}\lambda_k^{(i)T} \left[ \left( \Delta \mathbf{u}_k^{(i)} + \mathbf{O}_k^{(i-1)} \right) - \left( 1 - \beta^{(i)} \right) \Delta \mathbf{u}_A^{(i)} - \beta^{(i)} \Delta \mathbf{u}_B^{(i)} \right] \quad (4.11)$$

Where;  $\beta^{(i)} = \beta^{(i-1)} + \Delta \beta^{(i)}$

Assuming new penetration is almost zero, that is;  ${}^{t+\Delta t}\mathbf{P}_k^{(i)} \approx {}^{t+\Delta t}\mathbf{P}_C^{(i)}$

$$\Delta \beta^{(i)} \approx \frac{\mathbf{n}_r^T}{d_j^{(i-1)}} \left[ \left( \Delta \mathbf{u}_k^{(i)} + \mathbf{O}_k^{(i-1)} \right) - \left( 1 - \beta^{(i-1)} \right) \Delta \mathbf{u}_A^{(i)} - \beta^{(i-1)} \Delta \mathbf{u}_B^{(i)} \right] \quad (4.12)$$

Change in  $\beta$  is redefined by substituting Eq. (4.9) into Eq. (4.12);

$$\Delta \beta^{(i)} \approx \frac{\mathbf{n}_r^T}{d_j^{(i-1)}} \left[ \Delta \mathbf{u}_k^{(i)} + \mathbf{O}_k^{(i-1)} - \Delta \mathbf{u}_C^{(i)} \right] \quad (4.13)$$

This relation can be perceived from figure below.



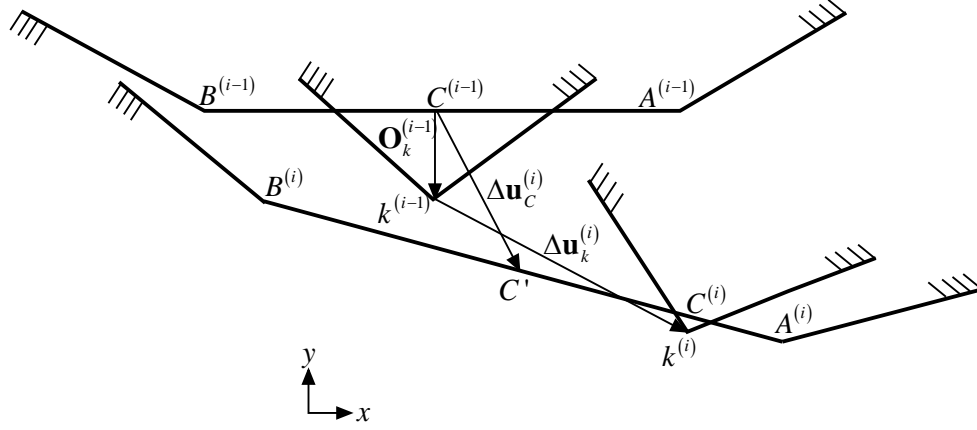


Figure 4.4 Geometry of contact in sliding condition

Change in contact force in local direction is given as follows.

$$\Delta \lambda_k^{(i)} = -\Delta \lambda_s^{(i)} \mathbf{n}_s \quad (4.14)$$

$${}^{t+\Delta t} \lambda_k^{(i)} = {}^{t+\Delta t} \lambda_k^{(i-1)} - \Delta \lambda_s^{(i)} \mathbf{n}_s \quad (4.15)$$

Potential is redefined by substituting Eq. (4.15) into Eq. (4.11);

$$\omega_k = \left( {}^{t+\Delta t} \lambda_k^{(i-1)} - \Delta \lambda_s^{(i)} \mathbf{n}_s \right)^T \left[ \left( \Delta \mathbf{u}_k^{(i)} + \mathbf{O}_k^{(i-1)} \right) - \left( 1 - \beta^{(i-1)} \right) \Delta \mathbf{u}_A^{(i)} - \beta^{(i-1)} \Delta \mathbf{u}_B^{(i)} \right] \quad (4.16)$$

The potential derived for sliding contact has the parameter  $\beta^{(i-1)}$ . This is due to simplify the problem. The parameter  $\beta^{(i)}$  can be used in Eq. (4.16) instead of  $\beta^{(i-1)}$ , however this will complicate the problem very much. Instead, the parameter  $\beta^{(i)}$  can be revised iteratively by using Eq. (4.12) or Eq. (4.13).

#### 4.4 Governing Finite Element Equations

A structural system has a potential  $\Pi$ . New potential is achieved by subtracting contact potential from the present potential.

$$\Pi_{new} = \Pi - \sum_k \omega_k \quad (4.17)$$

If  $\delta \Pi_{new} = 0$ , governing finite element equations will be;

$$\begin{bmatrix} {}^{t+\Delta t} \mathbf{K}^{(i-1)} & {}^{t+\Delta t} \mathbf{K}_{c^*}^{(i-1)} \\ \left( {}^{t+\Delta t} \mathbf{K}_{c^*}^{(i-1)} \right)^T & \mathbf{0} \end{bmatrix} \begin{bmatrix} \Delta \mathbf{U}^{(i)} \\ \Delta \boldsymbol{\lambda}^{(i)} \end{bmatrix} = \begin{bmatrix} {}^{t+\Delta t} \mathbf{F} \\ \mathbf{0} \end{bmatrix} - \begin{bmatrix} {}^{t+\Delta t} \mathbf{R}^{(i-1)} \\ \mathbf{0} \end{bmatrix} + \begin{bmatrix} {}^{t+\Delta t} \mathbf{R}_c^{(i-1)} \\ {}^{t+\Delta t} \mathbf{O}_c^{(i-1)} \end{bmatrix} \quad (4.18)$$

Where;

${}^{t+\Delta t} \mathbf{K}^{(i-1)}$  ; Tangential stiffness matrix of complete system (DDOF x DDOF)

${}^{t+\Delta t} \mathbf{K}_{c^*}^{(i-1)}$  ; Components of contact stiffness matrix  ${}^{t+\Delta t} \mathbf{K}_c^{(i-1)}$  (Dimension is changing according to contact conditions)

$\Delta \mathbf{U}^{(i)}$  ; Incremental displacements (DDOF x 1)

$\Delta \boldsymbol{\lambda}^{(i)}$  ; Incremental contact forces (CDOF x 1)

${}^{t+\Delta t} \mathbf{F}$  ; Total applied external loads (DDOF x 1)

${}^{t+\Delta t} \mathbf{R}^{(i-1)}$  ; Equivalent nodal forces (DDOF x 1)

${}^{t+\Delta t} \mathbf{R}_c^{(i-1)}$  ; Contact forces (DDOF x 1)

${}^{t+\Delta t} \mathbf{O}_c^{(i-1)}$  ; Overlaps (CDOF x 1)

DDOF ; Displacement degrees of freedom

CDOF ; Contact degrees of freedom

TDOF ; Total degrees of freedom (TDOF=DDOF+CDOF)

Governing finite element equations for sticking and sliding condition of small system defined before is given below, respectively.

$$\begin{bmatrix} & & & & & & & \\ & & & & & & & \\ & & & & & & & \\ & & & & & & & \\ & & & & & & & \\ & & & & & & & \\ & & & & & & & \\ & & & & & & & \\ -1 & 0 & 1-\beta^{(i-1)} & 0 & \beta^{(i-1)} & 0 & 0 & 0 \\ 0 & -1 & 0 & 1-\beta^{(i-1)} & 0 & \beta^{(i-1)} & 0 & 0 \end{bmatrix} \begin{bmatrix} -1 & 0 \\ 0 & -1 \\ 1-\beta^{(i-1)} & 0 \\ 0 & 1-\beta^{(i-1)} \\ \beta^{(i-1)} & 0 \\ 0 & \beta^{(i-1)} \\ 0 & 0 \\ 0 & 0 \end{bmatrix} \begin{bmatrix} \Delta u_{kx}^{(i)} \\ \Delta u_{ky}^{(i)} \\ \Delta u_{Ax}^{(i)} \\ \Delta u_{Ay}^{(i)} \\ \Delta u_{Bx}^{(i)} \\ \Delta u_{By}^{(i)} \\ \Delta \lambda_{kx}^{(i)} \\ \Delta \lambda_{ky}^{(i)} \end{bmatrix} = \begin{bmatrix} \\ \\ \\ 0 \\ 0 \end{bmatrix} - \begin{bmatrix} \\ \\ \\ 0 \\ 0 \end{bmatrix} + \begin{bmatrix} {}^{t+\Delta t}\Delta \lambda_{kx}^{(i-1)} \\ {}^{t+\Delta t}\Delta \lambda_{ky}^{(i-1)} \\ -(1-\beta^{(i-1)}) {}^{t+\Delta t}\Delta \lambda_{kx}^{(i-1)} \\ -(1-\beta^{(i-1)}) {}^{t+\Delta t}\Delta \lambda_{ky}^{(i-1)} \\ -\beta^{(i-1)} {}^{t+\Delta t}\Delta \lambda_{kx}^{(i-1)} \\ -\beta^{(i-1)} {}^{t+\Delta t}\Delta \lambda_{ky}^{(i-1)} \\ O_{kx}^{(i-1)} \\ O_{ky}^{(i-1)} \end{bmatrix} \quad (4.19a)$$

$$\begin{aligned}
& \begin{bmatrix} -n_{sx} & -n_{sy} & (1-\beta^{(i-1)})n_{sx} & (1-\beta^{(i-1)})n_{sy} & \beta^{(i-1)}n_{sx} & \beta^{(i-1)}n_{sy} & 0 \end{bmatrix} \begin{bmatrix} -n_{sx} \\ -n_{sy} \\ (1-\beta^{(i-1)})n_{sx} \\ (1-\beta^{(i-1)})n_{sy} \\ \beta^{(i-1)}n_{sx} \\ \beta^{(i-1)}n_{sy} \\ 0 \end{bmatrix} \begin{bmatrix} \Delta u_{kx}^{(i)} \\ \Delta u_{ky}^{(i)} \\ \Delta u_{Ax}^{(i)} \\ \Delta u_{Ay}^{(i)} \\ \Delta u_{Bx}^{(i)} \\ \Delta u_{By}^{(i)} \\ \Delta \lambda_s^{(i)} \end{bmatrix} = \begin{bmatrix} \\ \\ \\ 0 \\ 0 \end{bmatrix} - \begin{bmatrix} \\ \\ \\ 0 \\ 0 \end{bmatrix} + \begin{bmatrix} {}^{t+\Delta t}\Delta \lambda_{kx}^{(i-1)} \\ {}^{t+\Delta t}\Delta \lambda_{ky}^{(i-1)} \\ -(1-\beta^{(i-1)})^{t+\Delta t}\Delta \lambda_{kx}^{(i-1)} \\ -(1-\beta^{(i-1)})^{t+\Delta t}\Delta \lambda_{ky}^{(i-1)} \\ -\beta^{(i-1)t+\Delta t}\Delta \lambda_{kx}^{(i-1)} \\ -\beta^{(i-1)t+\Delta t}\Delta \lambda_{ky}^{(i-1)} \\ O_s^{(i-1)} \end{bmatrix} \quad (4.19b)
\end{aligned}$$

If two structures are not in contact, defined nodal point forces will be treated as unbalanced forces and minimized by nonlinear procedures. If two structures are in contact, nodes in contact are named as active nodes and nodes not in contact are named as passive nodes. Passive nodes are treated as unbalanced forces as explained above. In contrast, forces on active nodes are used to determine  ${}^{t+\Delta t}\mathbf{R}_c^{(i-1)}$ . In finite element equations above,  ${}^{t+\Delta t}\mathbf{R}_c^{(i-1)}$  is determined from  ${}^{t+\Delta t}\Delta\lambda^{(i)}$  for each iteration.

#### 4.5 Governing Finite Element Equations in Local Coordinates

A structure in contact can easily be solved by defined equations for pure sticking and sliding conditions. However, these equations are hard to apply as a computer code for solutions of both cases. Because, size of stiffness matrix changes for changing condition and coordinate transformation is needed.

Therefore, a general set of governing finite element equations is defined in Eq. (4.20a). In fact, this set is the same with the finite element equations of sticking condition Eq. (4.19a) but new definition can be easily converted for sliding condition as Eq. (4.20b). This conversion is done by making stiffness elements in r direction zero.

Besides, the use of finite element equations 4.19a and 4.19b, pushes solver to assume that structures are sticks together for first contact occurrence. However, solver should not make an assumption for initial contact occurrence if it uses Eq. (4.20a) and (4.20b).



Where;  $\mathbf{n}_s = \begin{bmatrix} n_{sx} \\ n_{sy} \end{bmatrix}$ ,  $\mathbf{n}_r = \begin{bmatrix} n_{rx} \\ n_{ry} \end{bmatrix}$

## 4.6 Contact Conditions

Contact mechanics needs some algorithms to apply the finite element equations as derived above. An algorithm is needed to decide whether the structures are in contact or not. After that, if structures are in contact, another algorithm is needed to decide whether structures stick together or slide. In the first algorithm, history of displacements and current position of the structures must be kept and some vector operations must be carried out. In the second algorithm, tractions at contact points must be determined and then decision on the type of contact condition must be made, accordingly.

### 4.6.1 Contact Search Algorithm

During the solution procedure, contact conditions can change in any iteration. A contact can occur for separate structures or a separation can occur for a bonded structures. Therefore, contact conditions must be checked in every iteration ( $i$ ). In this search, initial positions and contact conditions have to be known since the contact search is based on initial conditions.

Initially, it is assumed that the structures are disconnected. Therefore comparing the positions of structures in final iteration with initial positions of structures will give the contact conditions. Accordingly, a comparison is made between initial and final signs of cross products of vectors from contact node to the end nodes of target element. Besides, a most possible target element is defined for each contact node to minimize the calculation time for contact search algorithm. This determination is made by comparing the angles between vectors from the contact node to the end nodes of each target element. The target element having maximum angle is the most possible target element for the contact node.

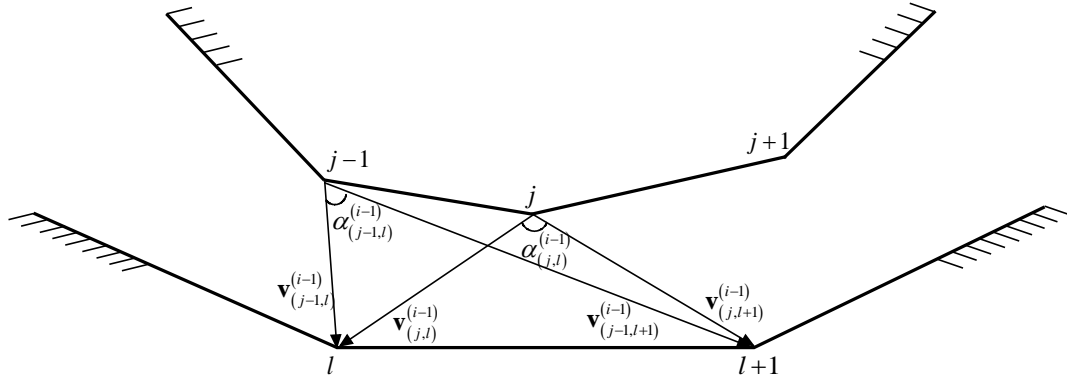


Figure 4.5 Vectors and angles for contact search

At  $(i-1)^{th}$  iteration, vectors from  $j^{th}$  contact node to  $l^{th}$  target node is denoted as  $\mathbf{v}_{(j,l)}^{(i-1)}$

.

Vectors from  $j^{th}$  contact node to each target node is calculated as;

$$\mathbf{v}_j^{(i-1)} = \begin{bmatrix} \mathbf{v}_{(j,l)}^{(i-1)} & \cdots & \mathbf{v}_{(j,l)}^{(i-1)} & \cdots & \mathbf{v}_{(j,note+1)}^{(i-1)} \end{bmatrix} = \mathbf{P}_t^{(i-1)} - \mathbf{P}_j^{(i-1)} \mathbf{n} \quad (4.21)$$

Where;

$\mathbf{P}_j^{(i-1)}$  ; Position vector of  $j^{th}$  contact node at  $(i-1)^{th}$  iteration

$\mathbf{P}_t^{(i-1)}$  ; Position vector of all target nodes

$$\mathbf{P}_t^{(i-1)} = \begin{bmatrix} \mathbf{P}_1^{(i-1)} & \cdots & \mathbf{P}_l^{(i-1)} & \cdots & \mathbf{P}_{note+1}^{(i-1)} \end{bmatrix}$$

$\mathbf{n}$  ; Unit normal vector

$$\mathbf{n} = \begin{bmatrix} 1 & \cdots & 1 \end{bmatrix}_{1 \times (note+1)}$$

$note$  ; Stands for number of target elements

Angle between adjacent vectors  $\alpha_{(j,l)}^{(i-1)}$  is calculated as described below. This angle can be regarded as the angle of  $j^{th}$  contact node with  $l^{th}$  target element which has end nodes  $l$  and  $l+1$ .

$$\alpha_{(j,l)}^{(i-1)} = \frac{\mathbf{v}_{(j,l)}^{(i-1)} \cdot \mathbf{v}_{(j,l+1)}^{(i-1)}}{\|\mathbf{v}_{(j,l)}^{(i-1)}\| \cdot \|\mathbf{v}_{(j,l+1)}^{(i-1)}\|} \quad (4.22)$$

The target element  $l$  having the maximum angle  $\max(\alpha_{(j,l)}^i)$  is the most possible target element for contact node  $j$ . A possible target element is calculated for each contact node to decrease the calculation time.

After determination of possible target elements. Sign of cross products  $sxp_{(j,l)}^{(i-1)}$  of vectors from each contact node to the end nodes of possible target element are calculated.

$$sxp_{(j,l)}^{(i-1)} = \text{sign}(\mathbf{v}_{(j,l)}^{(i-1)} \times \mathbf{v}_{(j,l+1)}^{(i-1)}) \quad (4.23)$$

If sign of cross products  $sxp_{(j,l)}^{(i-1)}$  of previously mentioned vectors changes during iteration, contact will occur at that contact node ( $j^{\text{th}}$  contact node) with that target element ( $l^{\text{th}}$  target element).

In other words, if summation of  $sxp_{(j,l)}^{(i-1)}$  at initial position and final position is zero there will be a contact.

$$ssxp_{(j,l)}^{(i-1)} = sxp_{(j,l)}^1 + sxp_{(j,l)}^{(i-1)} \quad (4.24)$$

#### 4.6.2 Contact Type Algorithm

Sticking and sliding contact types are different each other. As can be seen in Section 4.4, stiffness matrices are different. Therefore, contact type must be classified. This classification is based on traction forces applied on contact surface. These traction forces for contact node  $k$  can be determined from  ${}^{t+\Delta t}\lambda_k^{(i-1)}$ , as described in the following section. A frictional constant can be assumed for both kinetic and static case either as equal or different for each case. Contact type classification will change



according to the assumption made for frictional constants. Therefore, contact type classification is explained in the following two parts for each assumption.

#### 4.6.2.1 Case of Static Friction Being Equal to Kinetic Friction

Tangential traction force applied to a target element is  $T_t = {}^{t+\Delta t}\lambda_{kr}^{(i-1)}$ . Normal traction force applied to a target element is  $T_n = {}^{t+\Delta t}\lambda_{ks}^{(i-1)}$ . Assuming that the coefficient of static friction  $\mu_s$  is equal to coefficient of kinetic friction  $\mu_k$  ( $\mu_s = \mu_k = \mu$ ), frictional capacity of the contact will be equal to  $T_f = \mu T_n = \mu {}^{t+\Delta t}\lambda_{ks}^{(i-1)}$ .

If frictional capacity  $T_f$  is smaller than tangential traction  $T_t$ , the contact node slides on the target element. So, Eq. (4.20b) will be used for new iteration and tangential traction force will be made equal to frictional capacity.

If frictional capacity  $T_f$  is greater than tangential traction  $T_t$ , the contact node sticks to the target element. So, Eq. (4.20a) will be used for new iteration.

#### 4.6.2.2 Case of Static Friction Being Different from Kinetic Friction

Tangential traction force applied to a target element is  $T_t = {}^{t+\Delta t}\lambda_{kr}^{(i-1)}$ . Normal traction force applied to a target element is  $T_n = {}^{t+\Delta t}\lambda_{ks}^{(i-1)}$ . Assuming static coefficient of friction  $\mu_s$  not equals to kinetic coefficient of friction  $\mu_k$ , static and kinetic frictional capacity of the contact will be equal to  $T_{fs} = \mu_s {}^{t+\Delta t}\lambda_{ks}^{(i-1)}$  and  $T_{fk} = \mu_k {}^{t+\Delta t}\lambda_{ks}^{(i-1)}$ , respectively.

If the contact is previously in sliding condition and kinetic frictional capacity  $T_{fk}$  is smaller than tangential traction  $T_t$ , the contact node slides on the target element. So, Eq. (4.20b) will be used for new iteration and tangential traction force will be made equal to kinetic frictional capacity  $T_{fk}$ .

If contact is previously in sliding condition and kinetic frictional capacity  $T_{fk}$  is greater than tangential traction  $T_t$ , node sticks to the target element. So, Eq. (4.20a) will be used for new iteration.

If contact is previously in sticking condition and static frictional capacity  $T_{fs}$  is smaller than tangential traction  $T_t$ , the contact node slides on the target element. So, Eq. (4.20b) will be used for new iteration and tangential traction force will be made equal to kinetic frictional capacity  $T_{fk}$ .

If contact is previously in sticking condition and static frictional capacity  $T_{fs}$  is greater than tangential traction  $T_t$ , node sticks to the target element. So, Eq. (4.20a) will be used for new iteration.

## CHAPTER 5

### SOLUTION PROCEDURE

#### 5.1 General

Contact mechanics is composed of many different formulations with nested algorithms. First of all, discretized models of elastic solids are needed. In this thesis, one of the solids is selected as a truss structural system and modelled by using 2D bar elements (Chapter 2), the other solid is a cable formulated as explained in Chapter 3. Secondly, some algorithms are needed for contact mechanics to determine the condition of contact, i.e., a contact search algorithm (Section 4.6.1) and contact type algorithm (Section 4.6.2). Besides, some iterative algorithms should be used to imitate the post-tensioning operation by decreasing the cable length.

#### 5.2 Governing Set of Equations

Governing set of equations are given in Eq. (4.18). In this set of equations,  ${}^{t+\Delta t}\mathbf{K}^{(i-1)}$  is the tangent stiffness matrix of both the truss structural system and the cable. Dimension of this matrix is the total displacement degrees of freedom (DDOF) for the whole system. Stiffness of bar elements calculated by Eq. (2.12) and Eq. (2.13) and the stiffness of the cable element calculated by Eq. (3.24) are assembled into the tangent stiffness matrix  ${}^{t+\Delta t}\mathbf{K}^{(i-1)}$ . Contact stiffness matrix  ${}^{t+\Delta t}\mathbf{K}_c^{(i-1)}$  in Eq. (4.18) is determined from the defined potentials for both sticking and sliding conditions. Basically, contact stiffness matrix relates the displacements of target degrees of freedom (e.g. node A and B) and contact degrees of freedom (e.g. node k).

The total applied loads  ${}^{t+\Delta t}\mathbf{F}$  minus the equivalent nodal forces  ${}^{t+\Delta t}\mathbf{R}^{(i-1)}$  of the existing stresses in the structures is equal to the stiffness matrix of the structural system

multiplied by the deformations, as given in Eq. (2.7). However, the contact starts with the intrusion of the previously defined domains of the structures and this intrusion is rectified by the application of contact forces. Thus, additional contact forces  ${}^{t+\Delta t}\mathbf{R}_c^{(i-1)}$  applied to both structures.

There will be no contact forces  ${}^{t+\Delta t}\mathbf{R}_c^{(i-1)}$  and contact stiffness  ${}^{t+\Delta t}\mathbf{K}_c^{(i-1)}$  until the first intrusion is detected. After the first intrusion, the contact stiffness  ${}^{t+\Delta t}\mathbf{K}_c^{(i-1)}$  is formed and the change in displacements,  $\Delta\mathbf{U}^{(i)}$ , and change in the contact forces,  $\Delta\boldsymbol{\lambda}^{(i)}$ , corresponding to applied contact forces  ${}^{t+\Delta t}\mathbf{R}_c^{(i-1)}$  and overlaps  ${}^{t+\Delta t}\mathbf{O}_c^{(i-1)}$  of first intrusion are determined.

### 5.3 Solution Procedure

Inputs are determined as the initiation of the solution. Then, structure is initially solved for applied dead loads, because the post-tensioning application starts after positioning of the truss system. After solving the truss system initially, cable is solved for its initial length to determine its geometry. This geometry is needed for contact search algorithm. In this phase, it should be beware that structures are separate. Thus, initiation of the solution is finished.

Post-tensioning is applied by decreasing the cable length. So, the cable length is decreased and the cable is analyzed once again for its decreased length. Afterwards, the contact search is carried out to determine the contact occurrence as initial step of the iterations. If there is no contact, the cable length is decreased a bit more. If there is a contact, the stiffness of the structure and the stiffness of the cable is determined and assembled into the tangent stiffness matrix  ${}^{t+\Delta t}\mathbf{K}^{(i-1)}$ . Then, the contact forces  ${}^{t+\Delta t}\mathbf{R}_c^{(i-1)}$  are determined. Thus, the governing set of equations gets ready for solution.

After the application of constraints, change in displacements  $\Delta\mathbf{U}^{(i)}$  and change in contact forces  $\Delta\boldsymbol{\lambda}^{(i)}$  are determined and the location of the nodal points of truss system are revised. If the norm of change in displacements  $\Delta\mathbf{U}^{(i)}$  and/or change in the contact forces  $\Delta\boldsymbol{\lambda}^{(i)}$  are not smaller than a preset error tolerance, the cable is reanalyzed with

applied contact forces and the cable geometry is revised for the subsequent iteration. Otherwise, the solution is considered acceptable for the current unstressed length of the cable. The process is continued until target length or the post-tensioning force in the cable is reached.

A detailed description of the proposed solution procedure is also presented in the form of flow charts in Figure 5.1 -5.4, below.

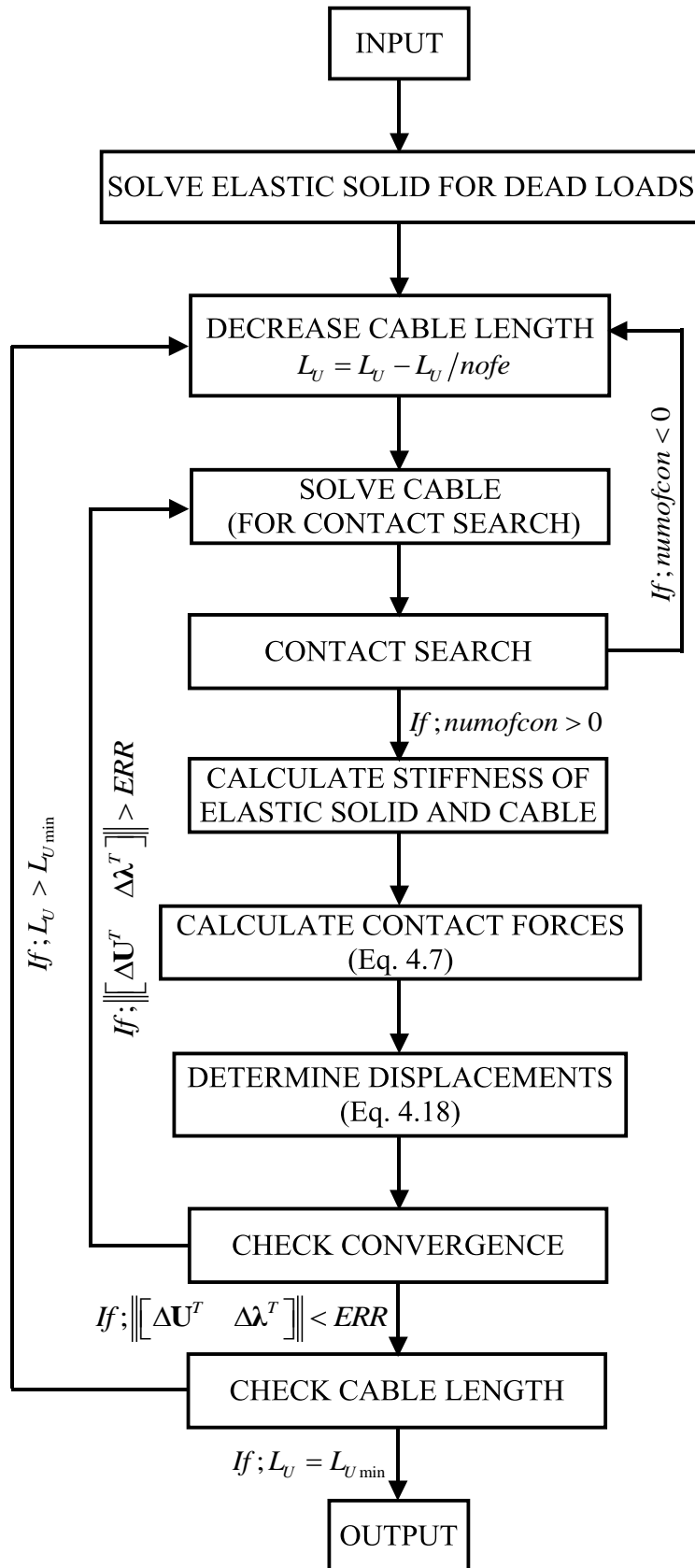


Figure 5.1 Flow diagram of the proposed algorithm

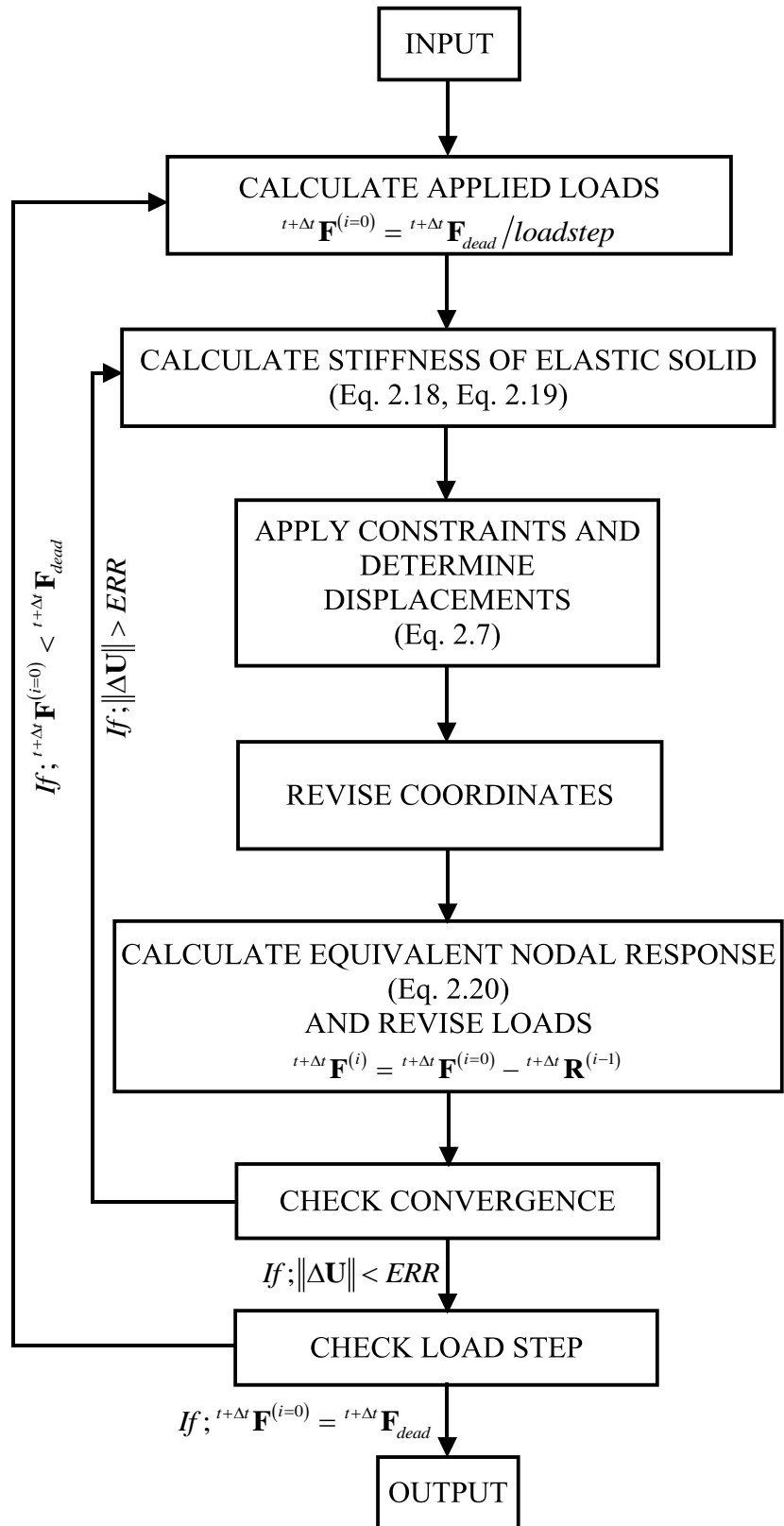


Figure 5.2 Flow chart for the analysis of the elastic structure

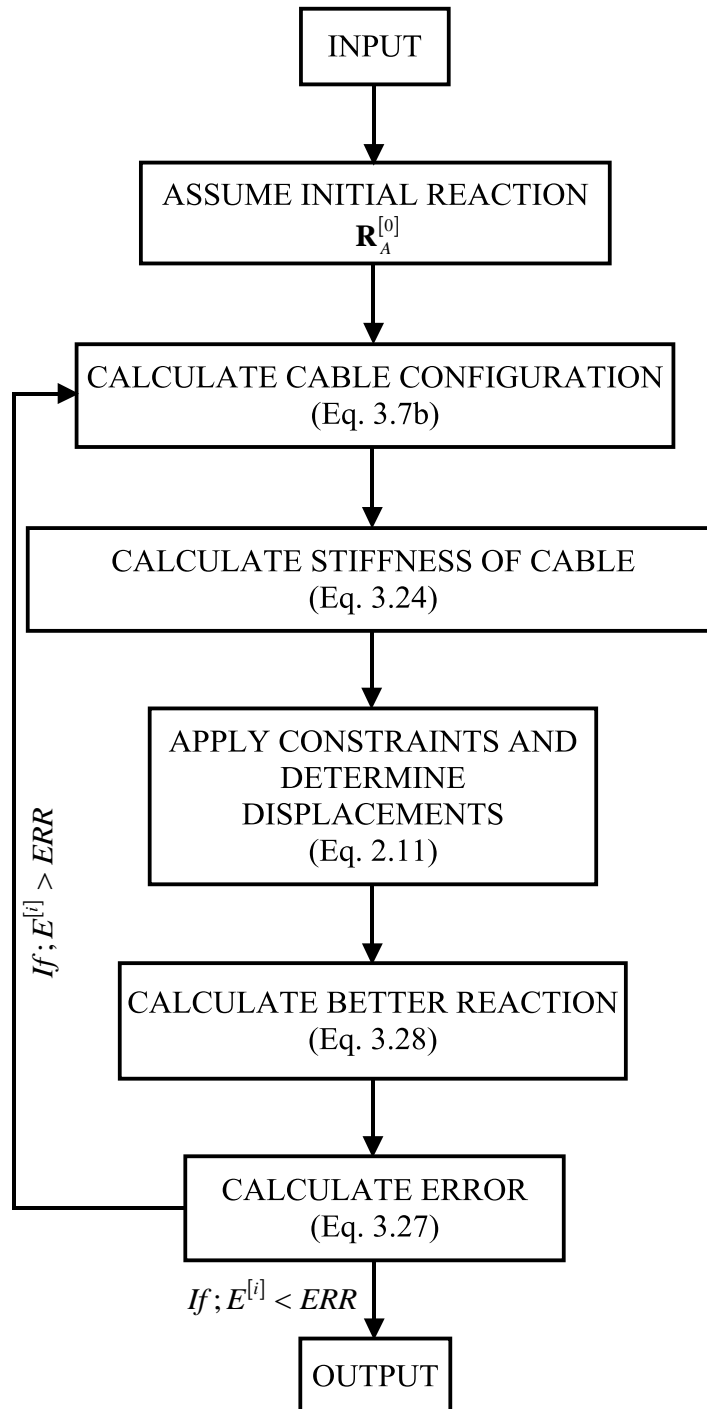


Figure 5.3 Flow chart for the analysis of cable



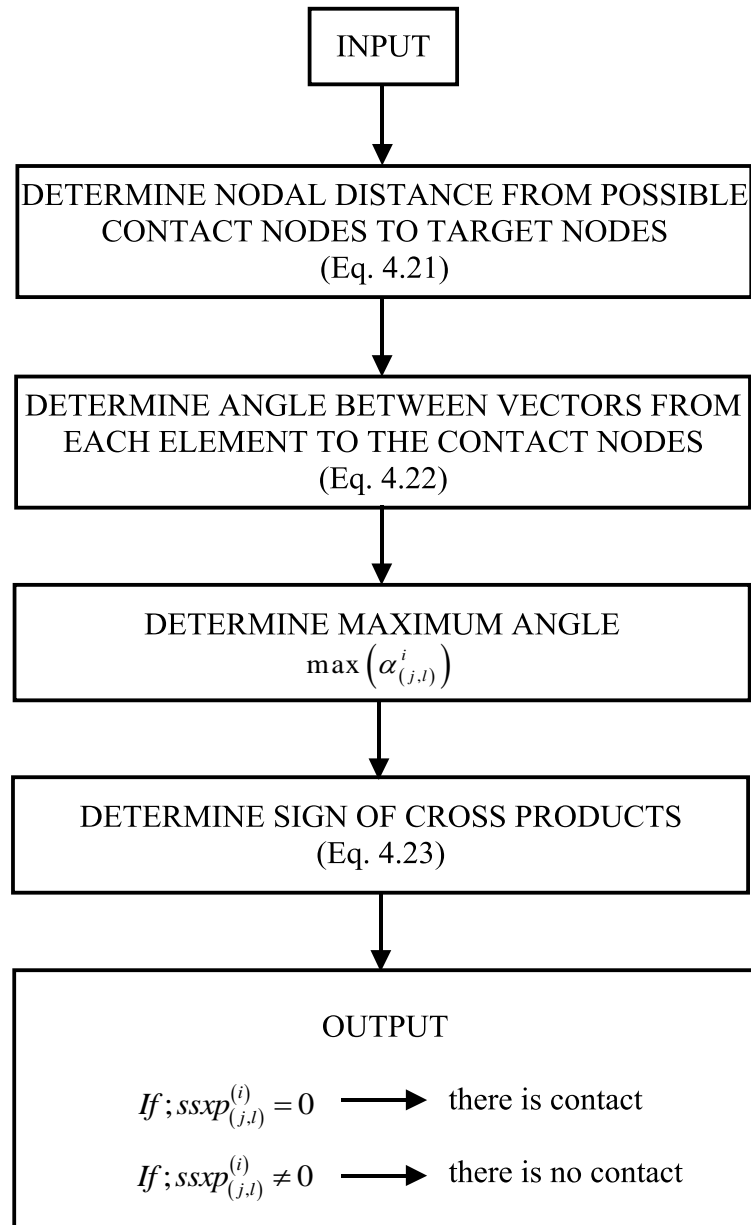


Figure 5.4 Flow chart for contact search



## CHAPTER 6

### VERIFICATION AND VALIDATION OF PROPOSED ALGORITHM

#### 6.1 General

A procedure for the solution of the interaction between a structure and a cable has been formulated. In order to check the validity and efficiency of the proposed algorithm, it is implemented into a special-purpose finite element code. A number of test problems are solved to check the major parameters of the algorithm. The results are compared with those obtained by the commercially available general-purpose finite element program ANSYS.

#### 6.2 Verification Test Structure

Verification model is selected as a steel truss structure having three contact nodes and a cable. Geometry of the model is shown below. The truss structure has a depth of 1.50m and a span of 12.0m. In order to simulate the real-life tensioning of the cable by a jacking operation, the length of the cable is gradually shortened by deleting the element of its numerical model one by one beginning from one of its ends.

The self-weight of both the cable and the truss structure is included in the analysis. Density of the cable is taken as  $7850 \text{ kgf/m}^3$  and the gravitational acceleration is taken as  $9.81 \text{ m/s}^2$ . In addition to its self-weight, the truss structure is also loaded by service load. This service load is represented by  $150.0 \text{ kN}$  point loads acting at each node of its top chord. All elements of the truss structure and the cable are defined as having a circular cross-section with a diameter of  $20 \text{ mm}$ . Rather flexible elements are selected for the truss structure to emphasize the geometrically nonlinear behavior of the structure.

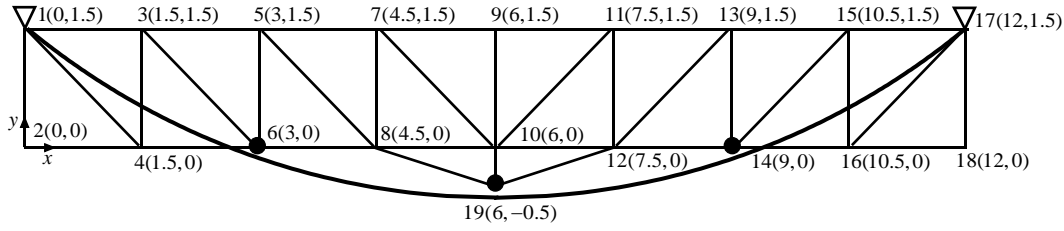


Figure 6.1 Geometry of the verification model

There are three major parameters and conditions affecting the behavior and the accuracy in the predicted results of the numerical simulation of nonlinear problems. These are the initial conditions, the number of finite elements in the model and the convergence criteria selected. These conditions have to be specified properly to have a correct result.

### 6.2.1 Initial Configuration of Cable

Initial unstressed length of the cable and its initial configuration are critical for the resulting solution. First of all, the initial unstressed length of cable must be long enough such that there will be no contact with the structure at the onset of simulation. Secondly, the cable must initially be in its natural shape under its own weight between the end nodes. However, in the commercial computer program ANSYS it is not easy to define the cable geometry in its natural state under its own weight. Therefore, two initial cable configurations (initial configurations I & II) are selected for verification by ANSYS, as shown below.

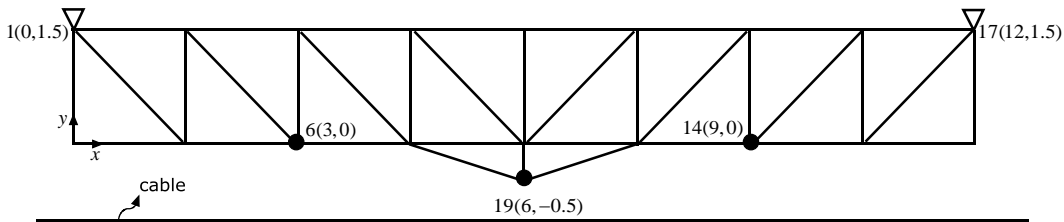


Figure 6.2 Initial cable configuration I

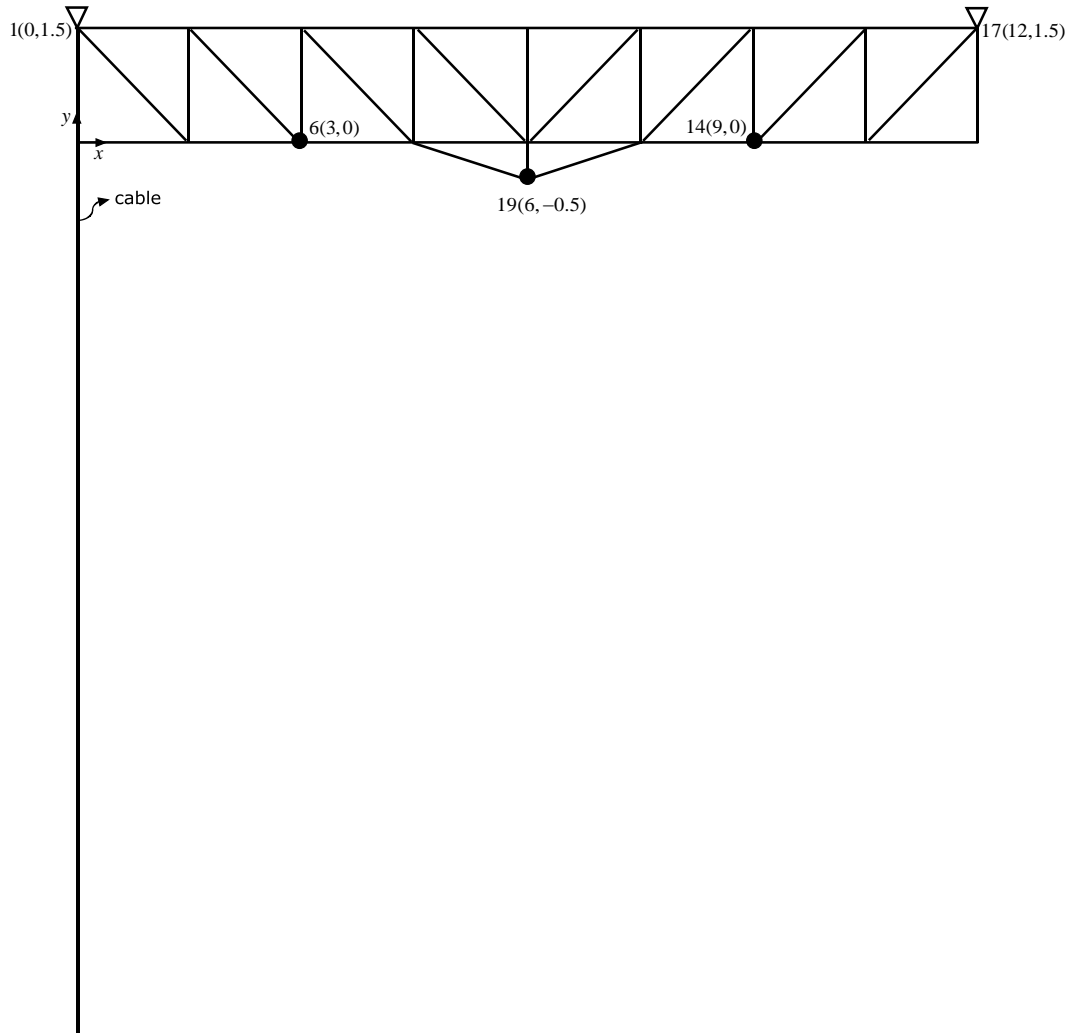


Figure 6.3 Initial cable configuration II

In both configurations, LINK10 is used to model cable element with tension only option. Truss elements are modelled with LINK180. Contact and target elements are modelled with CONTA175 and TARGE169, respectively.

#### 6.2.1.1 Some Theoretical Anticipations for Verification

It is known that, if the contact between the cable and the truss structure is frictionless, the cable tension at both ends (node 1 and node 17) will be equal. If both tensions are equal, the length of cable on either side of the contact node 19 will be equal and there will be no displacement at node 19 in the horizontal direction  $x$ .

This theoretically expected behavior is true if the cable is shortened from both sides at the same time and by the same amount in a frictionless environment. Therefore, the cable is started with its initial configuration I in ANSYS and a uniform temperature change is imposed, which satisfies the initial (13.2m) and final (12.6m) cable lengths to make the verification results comparable. The results of both simulations are shown below in Tables 6.1 and 6.2.

Table 6.1 Structural displacements for frictionless symmetric tensioning

Disp.	Proposed method		ANSYS		Difference (%)	
Node	$U_X$ (m)	$U_Y$ (m)	$U_X$ (m)	$U_Y$ (m)	$\Delta U_X$	$\Delta U_Y$
6	6.47E-04	-3.76E-03	6.47E-04	-3.76E-03	-0.06%	-0.14%
19	5.90E-14	-7.68E-03	-3.26E-14	-7.68E-03	---	-0.07%
14	-6.47E-04	-3.76E-03	-6.47E-04	-3.76E-03	-0.06%	-0.14%

Table 6.2 Contact forces for frictionless symmetric tensioning

Contact Forces	Proposed method		ANSYS		Difference (%)	
Node	$F_X$ (N)	$F_Y$ (N)	$F_X$ (N)	$F_Y$ (N)	$\Delta F_X$	$\Delta F_Y$
6	9.00E+04	2.76E+05	9.00E+04	2.76E+05	-0.01%	-0.05%
19	-4.52E-13	3.23E+05	0.00E+00	3.23E+05	---	-0.04%
14	-9.00E+04	2.76E+05	-9.00E+04	2.76E+05	-0.01%	-0.05%

It is seen that, both solutions have almost zero displacement at Node 19 in the horizontal direction, which is consistent with the expectations.

The initial and the final geometry of the structure predicted by ANSYS and the proposed procedure are illustrated below.

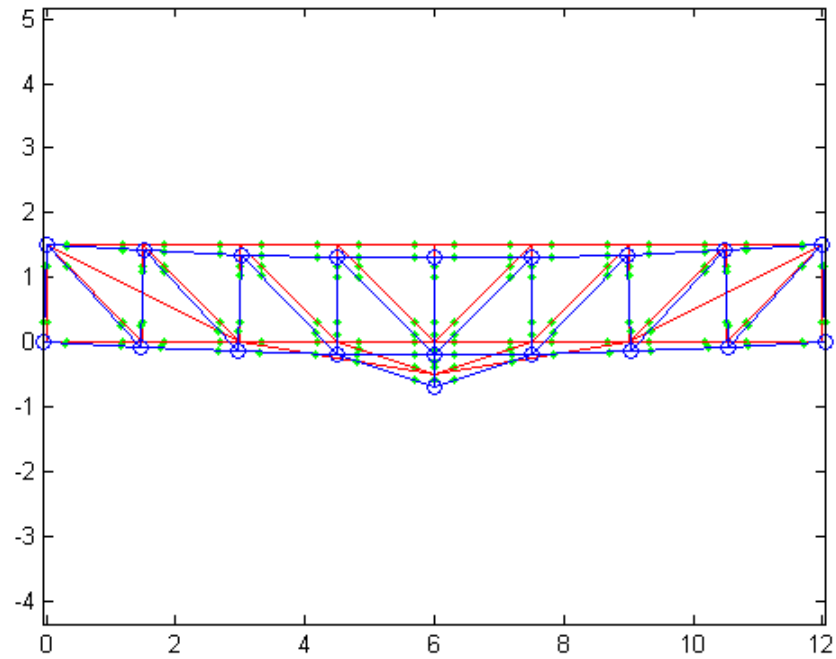


Figure 6.4 Initial and final geometry of the structure predicted by the proposed procedure

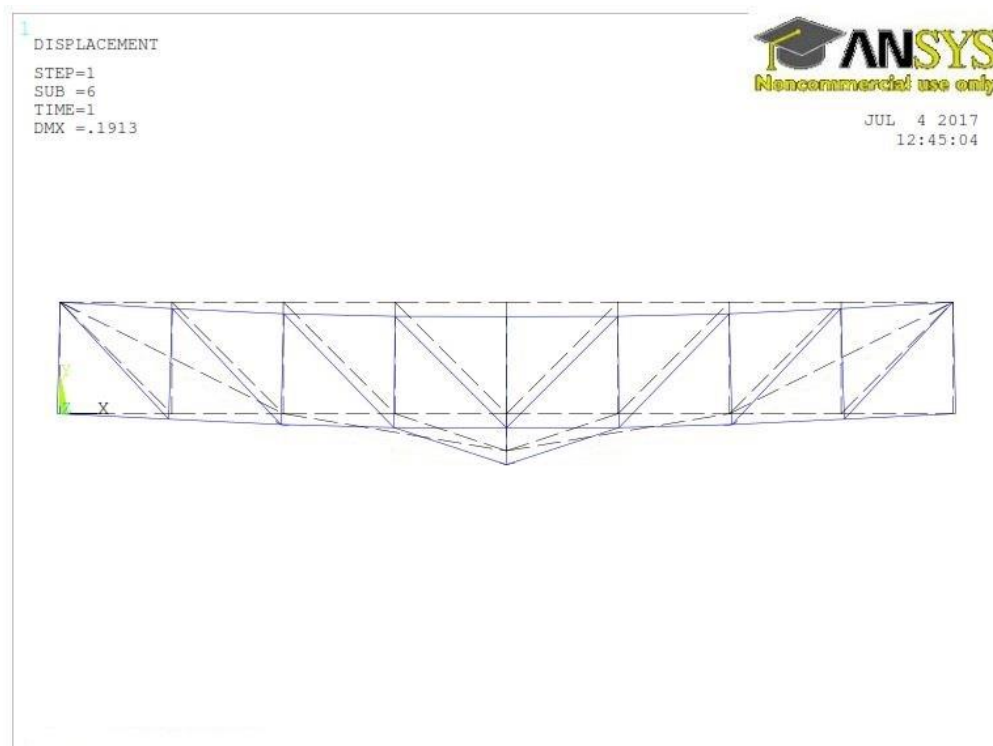


Figure 6.5 Initial and final geometry of the structure predicted by ANSYS

### 6.2.1.2 The Mesh Size and the Convergence Criteria Number of Cable Finite Elements and Maximum Allowable Error

The mesh size and the convergence criteria are very critical for the accuracy of the predicted results in the finite element solution of nonlinear problems. In the subject test structure, the truss system has 36 elements and this is sufficient due to the basic assumptions in its formulation. However, the cable must be divided into a number of sub-elements and the solution accuracy increases with the increased number of divisions. Therefore, the simulation have been repeated for different number of finite elements of the cable in a frictionless environment with a displacement based convergence criterion of 0.001. In this analysis, the initial configuration II is used for ANSYS. The results are listed in Table 6.3 below and shown graphically in Figures 6.6 and 6.7.

Table 6.3 Displacements of Node 19 for different number of cable finite elements

No. of Finite Elements	X-Displacement (m)		Y-Displacement (m)	
	Proposed Method	ANSYS	Proposed Method	ANSYS
200	-8.6800E-05	-2.8580E-05	-7.0465E-03	-7.0385E-03
300	-5.3900E-05	-2.2505E-05	-7.3160E-03	-7.3410E-03
500	-2.2380E-05	-1.5518E-04	-7.5960E-03	-7.6460E-03
1000	7.6450E-05	1.8963E-04	-7.6305E-03	-7.6376E-03
2000	3.3890E-05	6.9277E-05	-7.6805E-03	-7.7252E-03



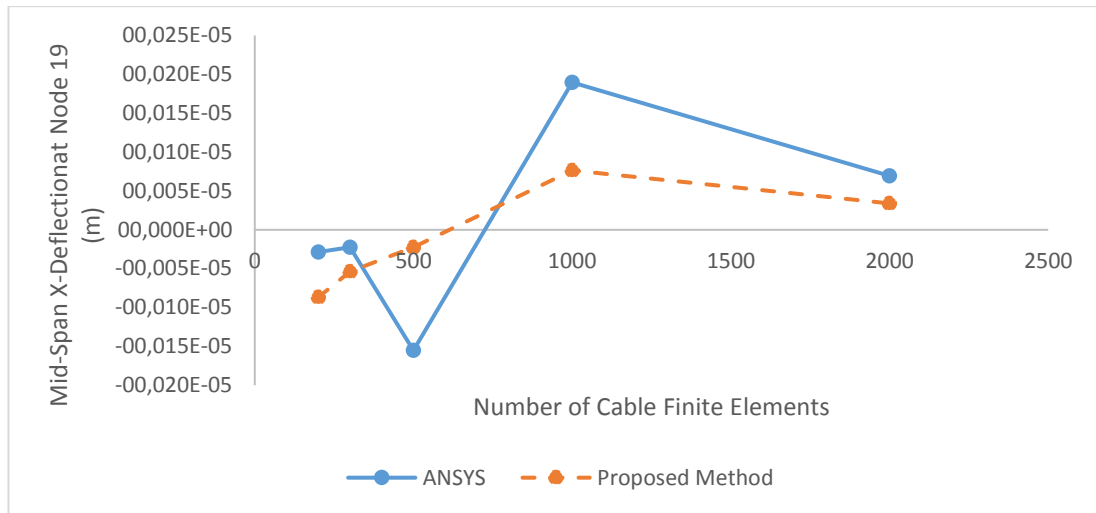


Figure 6.6 Displacement in X direction of Node 19 vs. the number of finite elements

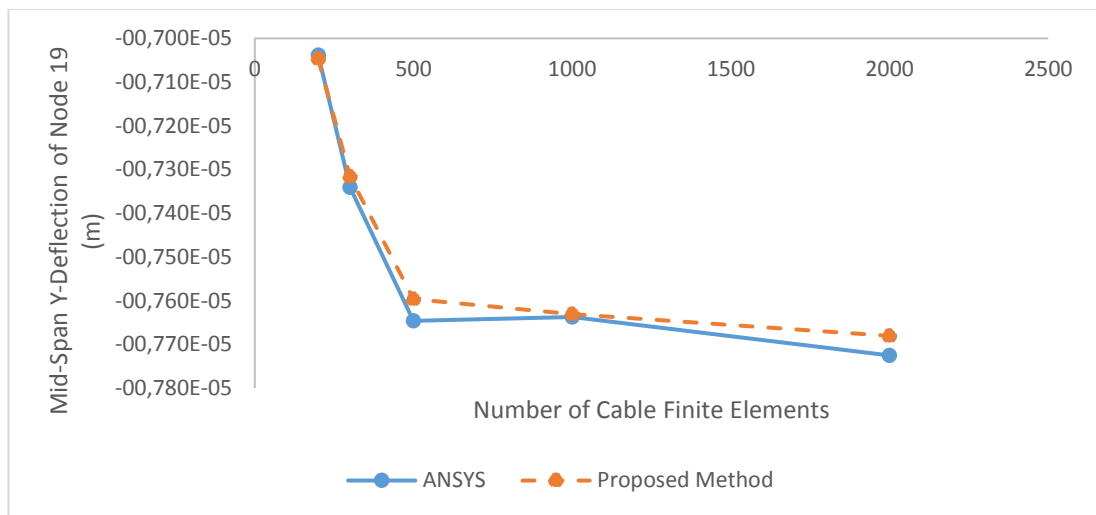


Figure 6.7 Displacement in Y direction of Node 19 vs. the number of finite elements

Using a course mesh with a small number of finite elements for the cable cannot converge to the expected mid-span deflection in x direction although the vertical deflection at mid-span is acceptable. Therefore, it is decided that a finite element mesh with 500 elements is sufficient for the cable for acceptable results.

A set of analyses is carried out for different levels of maximum allowable error with a mesh of 500 finite elements of the cable. The results are listed in Table 6.4 below and shown graphically in Figures 6.8 and 6.9.

Table 6.4 Displacements of node 19 for different maximum allowable error.

Maximum Allowable Error	X-Displacement (m)		Y-Displacement (m)	
	Proposed Method	ANSYS	Proposed Method	ANSYS
0.001	-5.3900E-05	-2.2505E-05	-7.3160E-03	-7.3410E-03
0.0001	-1.2800E-06	-3.7232E-06	-7.3667E-03	-7.3763E-03
0.00001	9.8000E-07	8.4505E-07	-7.3724E-03	-7.3780E-03
0.000001	3.9476E-08	7.1634E-08	-7.3733E-03	-7.3779E-03
0.0000001	8.5631E-09	-7.4702E-09	-7.3743E-03	-7.3778E-03

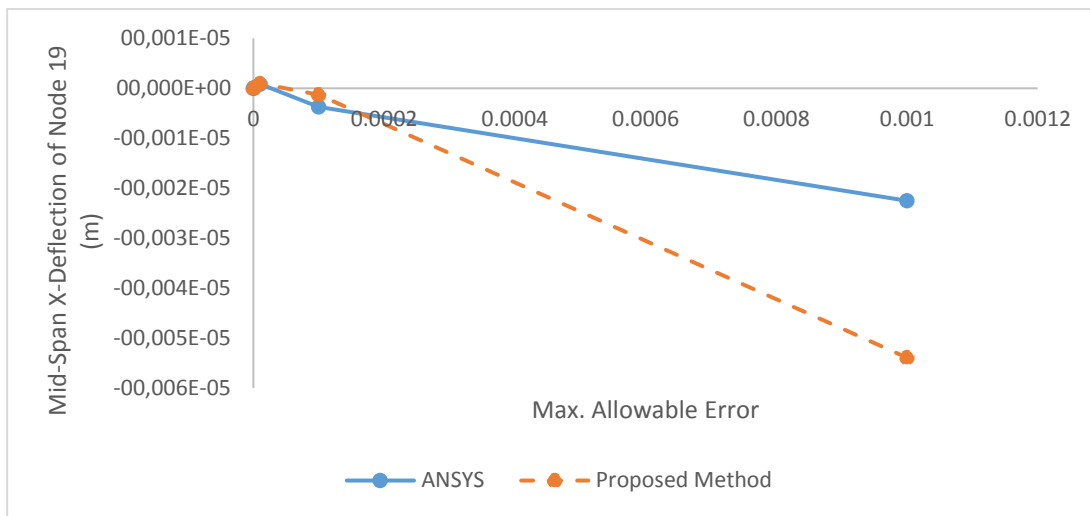


Figure 6.8 Displacement in X direction of Node 19 vs. the maximum allowable error.

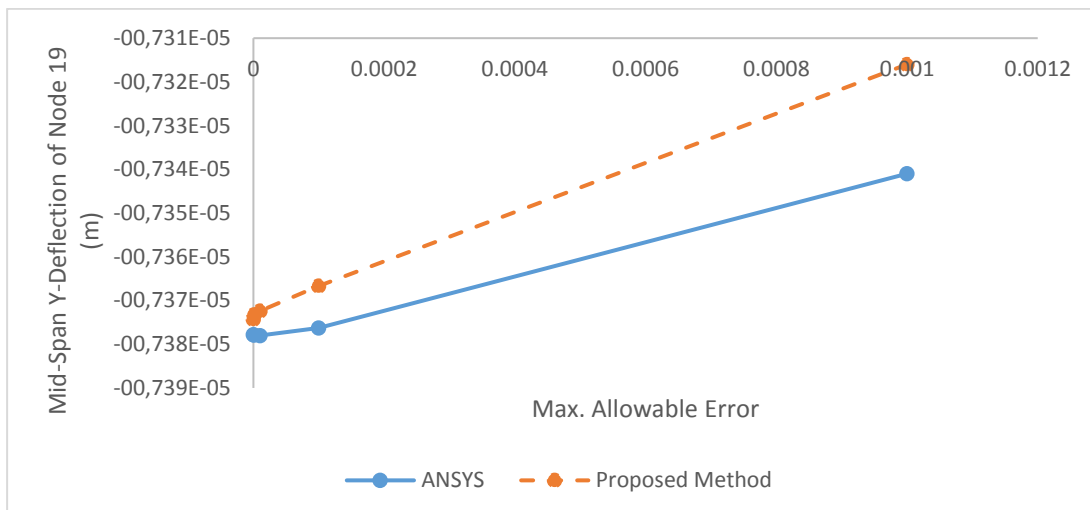


Figure 6.9 Displacement in Y direction of Node 19 vs. the maximum allowable error.

It seen that the mid-span deflection in X direction of Node 19 converges to zero by decreasing the maximum allowable error. It is decided that a convergence criterion of  $1.0 \times 10^{-5}$  m is sufficient for the Euclidian norm of the nodal displacements of all nodes in the model to have acceptable results from the analysis.

### 6.2.2 Frictional Environment

There will always be some friction between two contacting elements even if the magnitude of which may be very small. The magnitude of the contact friction is controlled by the specified coefficient of friction. The frictional capacity between two elements in contact is the normal force on the interface surface multiplied by the frictional coefficient.

In this study, only kinetic friction is considered assuming that the difference between the static and kinetic friction is negligible. The same test structure used for the frictionless environment is analyzed for different coefficients of friction defined for each of the contact nodes 6, 19 and 14. Initial configuration II is used for ANSYS and the bottom end of the cable is gradually forced by a series of prescribed displacements to its final position at Node 17. In contrast, cable is shortened by deleting finite elements beginning from Node 17, in proposed method. Thus, a jacking operation is simulated. In the following tables displacements (m) and contact forces (N) of each contact element for different coefficients of friction are given

Table 6.5 Displacements of Node 6 for different coefficients of friction

Frictional Coefficient	Proposed Method		ANSYS		Difference (%)
	X-Disp (m)	Y-Disp (m)	X-Disp (m)	Y-Disp (m)	
0.04	1.178E-03	-4.111E-03	1.188E-03	-4.125E-03	-0.39%
0.08	1.638E-03	-4.897E-03	1.626E-03	-4.871E-03	0.55%
0.12	2.064E-03	-5.614E-03	2.057E-03	-5.626E-03	-0.14%
0.16	2.477E-03	-6.379E-03	2.480E-03	-6.389E-03	-0.15%
0.2	2.896E-03	-7.160E-03	2.913E-03	-7.094E-03	0.71%
0.3	3.889E-03	-9.139E-03	3.902E-03	-9.126E-03	0.07%
0.4	4.933E-03	-1.100E-02	4.919E-03	-1.090E-02	0.85%

Table 6.6 Contact forces of Node 6 for different coefficients of friction

Frictional Coefficient	Proposed Method		ANSYS		Difference (%)
	F <sub>X</sub> (N)	F <sub>Y</sub> (N)	F <sub>X</sub> (N)	F <sub>Y</sub> (N)	
0.04	1.002E+05	2.709E+05	1.003E+05	2.704E+05	0.15%
0.08	1.100E+05	2.631E+05	1.099E+05	2.636E+05	-0.12%
0.12	1.196E+05	2.577E+05	1.191E+05	2.568E+05	0.36%
0.16	1.278E+05	2.491E+05	1.281E+05	2.501E+05	-0.36%
0.2	1.369E+05	2.435E+05	1.369E+05	2.439E+05	-0.14%
0.3	1.573E+05	2.270E+05	1.577E+05	2.272E+05	-0.16%
0.4	1.775E+05	2.128E+05	1.771E+05	2.125E+05	0.19%

These two tables show that increasing frictional constant increases both displacement and contact force at Node 6 in X direction. In contrast, this increase decreases both displacement and contact force at Node 6 in Y direction.

Table 6.7 Displacements of Node 19 for different coefficients of friction

Frictional Coefficient	Proposed Method		ANSYS		Difference (%)
	X-Disp (m)	Y-Disp (m)	X-Disp (m)	Y-Disp (m)	
0.04	9.371E-04	-7.270E-03	9.360E-04	-7.275E-03	-0.06%
0.08	1.859E-03	-7.200E-03	1.871E-03	-7.191E-03	0.07%
0.12	2.800E-03	-7.139E-03	2.804E-03	-7.125E-03	0.15%
0.16	3.744E-03	-7.070E-03	3.737E-03	-7.078E-03	-0.05%
0.2	4.668E-03	-7.050E-03	4.660E-03	-7.053E-03	0.02%
0.3	7.024E-03	-7.042E-03	6.989E-03	-7.055E-03	0.15%
0.4	9.320E-03	-7.021E-03	9.288E-03	-7.030E-03	0.17%

Table 6.8 Contact forces of Node 19 for different coefficients of friction

Frictional Coefficient	Proposed Method		ANSYS		Difference (%)
	F <sub>X</sub> (N)	F <sub>Y</sub> (N)	F <sub>X</sub> (N)	F <sub>Y</sub> (N)	
0.04	1.280E+04	3.229E+05	1.277E+04	3.227E+05	0.08%
0.08	2.573E+04	3.234E+05	2.551E+04	3.231E+05	0.08%
0.12	3.813E+04	3.230E+05	3.824E+04	3.235E+05	-0.13%
0.16	5.110E+04	3.233E+05	5.094E+04	3.237E+05	-0.11%
0.2	6.362E+04	3.239E+05	6.350E+04	3.238E+05	0.03%
0.3	9.539E+04	3.235E+05	9.520E+04	3.240E+05	-0.13%
0.4	1.262E+05	3.236E+05	1.264E+05	3.233E+05	0.06%

An increase is obvious for both displacement and contact force for Node 19 in X direction. However, there is almost no change in Y direction.

Table 6.9 Displacements of node 14 for different coefficients of friction

Frictional Coefficient	Proposed Method		ANSYS		Difference (%)
	X-Disp (m)	Y-Disp (m)	X-Disp (m)	Y-Disp (m)	
0.04	-3.039E-04	-2.579E-03	-3.062E-04	-2.561E-03	0.66%
0.08	1.362E-04	-1.749E-03	1.359E-04	-1.746E-03	0.17%
0.12	5.838E-04	-9.429E-04	5.850E-04	-9.416E-04	0.05%
0.16	1.050E-03	-1.462E-04	1.041E-03	-1.487E-04	0.78%
0.2	1.504E-03	5.626E-04	1.521E-03	5.774E-04	-1.27%
0.3	2.720E-03	2.569E-03	2.693E-03	2.535E-03	1.14%
0.4	3.928E-03	4.489E-03	3.909E-03	4.452E-03	0.69%

Table 6.10 Contact forces of node 14 for different coefficients of friction

Frictional Coefficient	Proposed Method		ANSYS		Difference (%)
	F <sub>X</sub> (N)	F <sub>Y</sub> (N)	F <sub>X</sub> (N)	F <sub>Y</sub> (N)	
0.04	-8.020E+04	2.834E+05	-8.048E+04	2.840E+05	-0.24%
0.08	-7.072E+04	2.919E+05	-7.018E+04	2.908E+05	0.42%
0.12	-5.932E+04	2.970E+05	-5.964E+04	2.975E+05	-0.20%
0.16	-4.855E+04	3.058E+05	-4.885E+04	3.044E+05	0.45%
0.2	-3.782E+04	3.134E+05	-3.869E+04	3.113E+05	0.62%
0.3	-9.320E+03	3.262E+05	-9.194E+03	3.287E+05	-0.76%
0.4	2.121E+04	3.451E+05	2.100E+04	3.466E+05	-0.43%

Both, the displacement and contact force increase with increasing frictional constant in either direction at Node 14.

#### 6.2.2.1 Cable Tension for Different Frictional Coefficients

The tension at cable ends is expected to be different for any case except for the frictionless case (Section 6.2.1.1). Tension at the end where the jacking operation side is greater than the other side. Because accumulation of friction forces makes the tension of cable on the pulling side greater. Variation of tensile force at the cable ends are shown below for varying coefficients of friction.

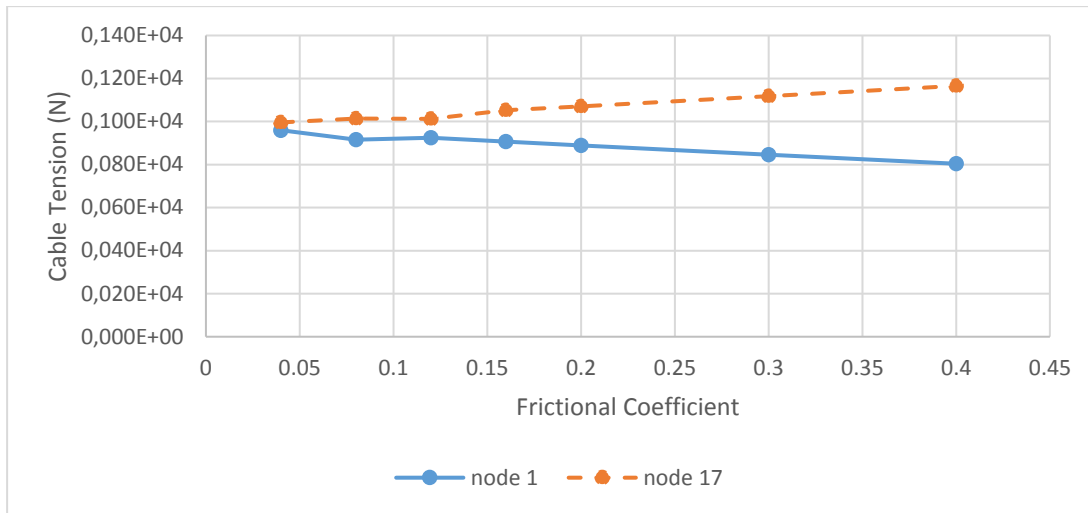


Figure 6.10 Cable tensions vs coefficients of friction

Cable tension at the ends is almost identical for smaller coefficient of friction. The difference between tensions at cable ends is increasing with the increasing coefficient of friction. Moreover, while the tension at anchored side is decreasing, the tension at the jacking side is increasing with increasing coefficient of friction.

### 6.2.3 Altered Cable Lengths

In the verification model, the coefficient of friction is assumed to be 0.2 and the cable is started with an initial unstressed length of 13.2m. Later, it is gradually decreased to 12.6m in the course of simulation. In the proposed method, this shortening is made by deleting the cable finite elements one by one starting with the element adjacent to Node 17 whereas a cable having the final unstressed length is placed in the initial configuration II and its free end is forced to its target location on the structure by gradually applied prescribed displacements in ANSYS. The mid-span displacement at Node 19 and the cable tension at nodes 1 and 17 are given below for different cable lengths. The difference in cable tension and mid-span deflection between the predictions of the proposed scheme and ANSYS is negligibly small for slack cables and increases with the increasing cable tension although it is still very small.

Table 6.11 Results for different final lengths of cable

Cable Length	Mid-span Disp. (m)	Difference Mid-span Disp.	Cable Tension (N)		Difference Cable Tension	
			Node 1	Node 17	Node 1	Node 17
13.20	1.8537E-01	0.000%	2.4829E+02	2.4829E+02	0.091%	0.045%
13.10	1.8537E-01	0.000%	2.5388E+02	2.5388E+02	-0.092%	-0.092%
13.00	1.8537E-01	0.000%	2.6832E+02	2.7026E+02	-0.005%	0.041%
12.99	1.8537E-01	0.000%	2.9109E+02	2.9811E+02	-0.061%	-0.042%
12.98	1.8536E-01	0.000%	3.2381E+02	3.3822E+02	0.011%	-0.015%
12.97	1.8535E-01	0.000%	3.7657E+02	4.0289E+02	0.018%	-0.083%
12.96	1.8533E-01	0.000%	4.8337E+02	5.3378E+02	0.027%	-0.030%
12.95	1.8524E-01	0.000%	9.5082E+02	1.1069E+03	-0.012%	-0.104%
12.90	1.6227E-01	0.000%	1.1874E+05	1.4521E+05	-0.057%	0.022%
12.80	1.1228E-01	-0.009%	3.7177E+05	4.5221E+05	-0.028%	-0.127%
12.70	6.0703E-02	0.012%	6.2835E+05	7.6023E+05	0.150%	-0.164%
12.60	8.4534E-03	-0.023%	8.8876E+05	1.0697E+06	0.310%	-0.274%

Gradual change in mid-span displacement and cable tension is shown below for changing length of cable.

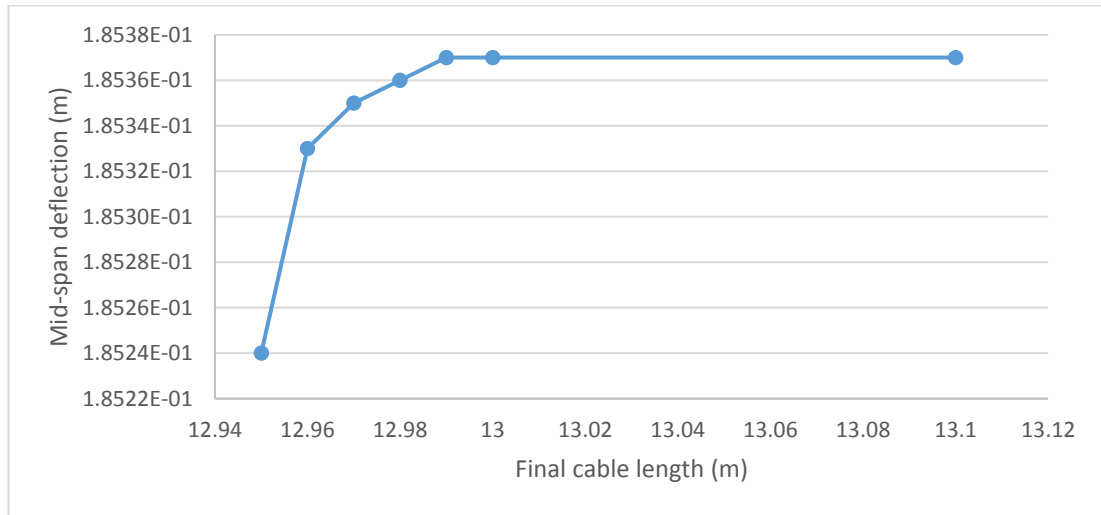


Figure 6.11 Mid-span displacement vs. final cable length

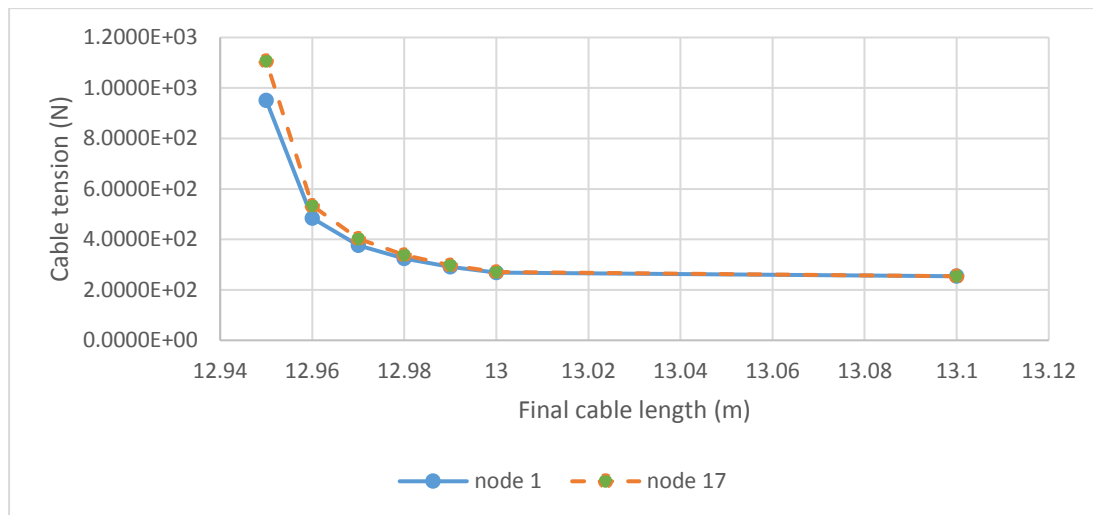


Figure 6.12 Cable tension vs. final cable length



## **CHAPTER 7**

### **CASE STUDIES**

#### **7.1 General**

In order to show the use of the proposed procedure in a practical situation, strengthening of an existing truss structure often encountered in structural engineering practice is selected as a case. The ultimate goal is, for one reason or another, to increase the load carrying capacity of the given structure.

The existing structure is defined and alternative approaches to the solution of the problem are described below from an engineer's point of view. It is assumed that a post-tensioning by cables is selected by the engineer as the most feasible and practical solution to the task of strengthening the given structure. The numerical simulation of alternative operations of post-tensioning is carried out using the procedure proposed and outlined in this thesis. Finally, a brief discussion of the simulation results is given.

#### **7.2 Description of the Sample Truss Structure**

A 2D steel roof truss structure is selected for post-tensioning. The plane truss is one of the individual trusses of a space frame roof structure in which a number of such trusses are placed parallel to each other with a spacing of 3.0m. The displacements at one end is restrained and the other end is free to slide in the horizontal direction, as shown in Figure 7.1. The structure has a total span length of 75.0m and consist of 25 panels with a uniform length of 3.0m each. The roof structure is 4.0m deep and each layer is 2.0m high. In its existing state, it is composed of 179 bar elements. Element labeling scheme is given in Appendix 1.

Besides the usual self-weight, the roof structure is subject to a top cover load of 22.65 kgf/m<sup>2</sup> and the bottom cover load of 11.33 kgf/m<sup>2</sup>. In addition, the structure is to resist

a snow load of 169.89 kg/m<sup>2</sup>. Considering the spacing of 3.0m between such trusses in the roof structure, the loading corresponds to a nodal cover load of 2.0 kN/node along the top chord and 1.0 kN/node along the bottom chord. The snow load along the top chord is 15.0 kN/node. These loads are factored loads for LRFD format. Initially, no other load is acting on the structure.

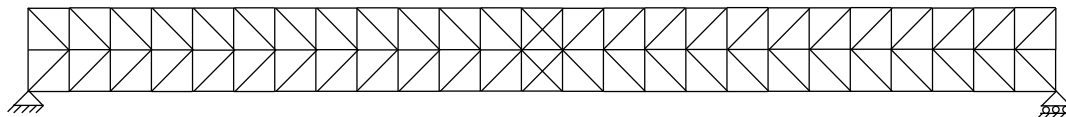


Figure 7.1 Geometry of structure

### 7.2.1 Original Design of the Truss Structure

The initial design of the steel truss with the given loads was based on the requirements of the ANSI/AISC 360-10 code for steel structures. All of the elements of the structure are circular hollow sections and made of S235 steel. The sections used in the model are grouped and labeled as Type1 through Type5, as defined in Table 7.1 below. The top layer member are of Type1, the bottom layer members are of Type2 and middle layer members are of Type3. The diagonals in the first 5 panels from each end are of Type4 and all other diagonals and posts are of Type5 members. A list of the element types for each member and the element type descriptions are given in

and Appendix 4. Initially, the resulting stresses (see Appendix 5) are at limit state for elements 75, 82, 98 and 105 which are the bottom chord members near the mid-span.

Table 7.1 Circular pipe sections used in the structure

Name	Outer Diameter (mm)	Inner Diameter (mm)	Sectional Area (mm <sup>2</sup> )
Type1	219.1	195.1	7807.486
Type2	219.1	199.1	6569.07
Type3	88.9	80.9	1066.885
Type4	139.7	127.7	2520.186
Type5	139.7	131.7	1705.256

### 7.2.2 Case I: Internal Post-tensioning

The objective is to strengthen and increase the load carrying capacity of the structure with post-tensioning application. Two cables having 42 mm nominal diameter and  $1030 \text{ mm}^2$  metallic area and a total breaking force of 2840 kN is used for this purpose. Although the post-tensioning can be applied to the structure in its native form, a number of members are added to the structure to increase the eccentricity (Appendix 2) and, consequently, the effectiveness of the post-tensioning operation. Final geometry of the truss system with the additional members and the initial state of the post-tensioning cable is shown in Figure 7.2. The highlighted nodes are the contact nodes at which the structure and the cable interacts. It is assumed that the friction at contact nodes is negligibly small.

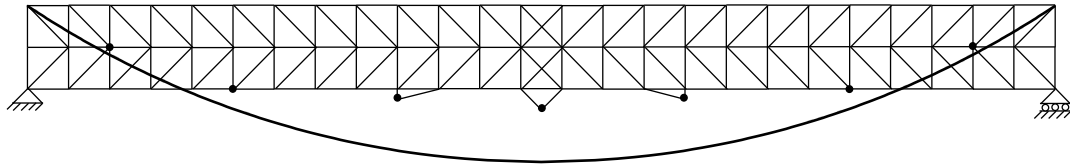


Figure 7.2 Geometry of the structure for Case I

The cable has an initial unstressed length of 80.0m and it is modelled with 2000 elements. Post-tensioning operation is started with the cover load already on the structure but no snow load and performed by decreasing the cable length until the strength limit state in the structure is reached. The limit state is reached after deleting 106 of the cable finite elements at one end. In this limit state, four truss members become critically stressed and they are the same elements (members 75, 82, 98 and 105) at the bottom chord of the truss structure (Appendix 6). However, this time they are in compression. At this state, the unstressed cable length is 75.76m and the cable tension is 1582 kN.

After post-tensioning operation, the snow load is applied on the structure. It is gradually increased until another strength limit state is reached. Finally, a critical compressive stress level is reached in the elements 3, 59, 66, 73, 103, 110, 117 and 173 of the top chord of truss (Appendix 7). At this state, the nodal snow load is 28 kN/node and the cable tension becomes 1915 kN. Thus, the structure is capable

resisting a snow load of 28 kN/node as opposed to 15 kN/node in its original state. This amounts to some 87% increase in snow load capacity or 72% increase in total load-carrying capacity of the structure.

### 7.2.3 Case II: External Post-tensioning with Nearby Anchorage

It is a customary practice to apply post-tensioning to an existing member or a structure by fixing the cable ends on the structure itself. This provides post-tensioning by itself. Although it is more beneficial to fix the cable ends on an external rigid structure or ground them as in the case of suspension bridges, this is, in general, not possible and/or practical for structures supported by long columns.

An alternative anchoring option for the post-tensioning cable is considered in this case study. Assuming that a given truss structure is supported by R/C columns and the column cross-sectional dimensions are such that anchoring the cable ends on the columns is possible, external post-tensioning operation can be used for strengthening. This way, the cable tension is transferred to an external body, which will reduce the level of straining in most of the truss members. Therefore, the cable end are assumed to be anchored at some points near the support locations of the structure as shown in Figure 7.3. However, the axial compressive force in the end posts are expected to be critically high. Straining in the members of the structure near the support locations are also expected to be high. Because of this anticipated behavior the vertical end posts of the truss structure are reinforced with additional circular hollow sections having a cross-sectional area of 200 cm<sup>2</sup>.

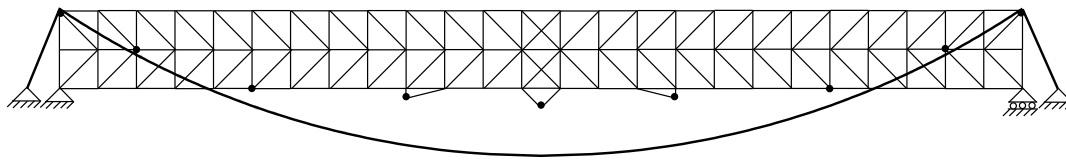


Figure 7.3 Geometry of structure in Case II

The distance between the cable anchorage points and the structural support locations is taken as 0.30 m, which is reasonable for practical applications. The post-tensioning cable is 88.0 m long and mathematically modelled by 2200 finite elements.

The simulation of the strengthening procedure by external post-tensioning of the structure follows the same steps as in the case of internal post-tensioning of Case I. With the cover load on the structure, the cable length is reduced to 83.76 m. At this state, the elements 75, 82, 98 and 105 of the bottom chord are in limit state (Appendix 8 and the tension in the cable is 1543 kN.

Snow load is then applied and gradually increased until the elements in the top chord reaches a strength limit state (Appendix 9). In this final state, the snow load is 30.0 kN/node and the cable tension is 1886 kN. Thus, the snow load capacity is increased by 100% or the total load carrying capacity is increased by 83%.

#### **7.2.4 Case III External Post-tensioning with Remote Anchorage**

In order to see the influence on the effectiveness of the guy cable orientation, Case II is repeated with the cable ends anchored at a distance of 4.0m away from the supports of the truss structure. Initial length of the cable is taken as 90.0 m and it is mathematically modelled using 2250 finite elements. In the first phase of strengthening the structure is post-tensioned by reducing the cable length down to 87.0 m. In this state, the elements 75, 82, 98 and 105 are in limit state as in Case II (Appendix 10) and the cable tension is 1618 kN. In the second phase, snow load is applied and gradually increased until the elements in the top chord reaches a strength limit state (Appendix 11). At the end of this second phase, the snow load on the structure is 60kN/node and the cable tension is 2462 kN. Hence, the snow load capacity is increased by 300% with this orientation of the guy cables.

### **7.3 Discussion on the Results of Case Studies**

The numerical procedure proposed in this study for the simulation of post-tensioning operations on structures is used for strengthening of an existing steel truss structure.

Two alternative options are considered for post-tensioning of the existing structure. For situations where the space around the structure is limited, usual procedure of internal post-tensioning as it is widely used for reinforced concrete members is the only choice. In this type of post-tensioning application, the tensile force created in the

cable by the jacking operation is totally absorbed by the structure. Therefore, the effectiveness of the operation is expected to be limited and the results are in line with this anticipation.

In most of the practical situations, such structures are usually supported by an underlying base structure or abutments in which there is always some room for anchoring the cable ends at some points outside the subject structure. In such cases, an external post-tensioning is practical and feasible. Part of the resulting cable tension of the post-tensioning operation is transferred to the other supporting structure. This way, the amount of additional straining in the structure due to cable tension to be absorbed by the subject structure is expected to be reduced. The simulation results prove this anticipation to be true and, as a result, the amount of gain in the load carrying capacity of the structure goes up to 300% as opposed to a relatively limited gain of 72% in the case of internal post-tensioning. It is also seen that the level of effectiveness of the external post-tensioning operation is closely related to the inclination of the guy cable which in turn depends on the distance of the cable anchorage point from the support of the subject structure. It is further seen that an optimum situation for the effectiveness of the post-tensioning operation is when the inclination of the guy cable or the location of the cable anchorage point is such that the reaction of the cable on the end post of the subject structure is a vertical compression.

## **CHAPTER 8**

### **SUMMARY AND CONCLUSIONS**

#### **8.1 Summary**

In this thesis, an analysis procedure is formulated and proposed for the cable-structure interaction problem encountered in various practical applications of structural mechanics. Although there are several approaches to the analysis of cables, only a few study is available in the literature for their interaction with other structures taking into account the complex contact problem between them. The algorithms proposed by the researchers are usually for a multi-segment continuous cable assuming a frictionless environment and stationary support locations. The algorithm proposed in this thesis is for a multi-segment continuous cable supported with frictional and non-stationary elastic supports.

The proposed approach couples the elastic structural system with the cable by considering the contact conditions and the resulting contact forces between them. For this purpose a nonlinear cable and a geometrically nonlinear bar element have been formulated in addition to a contact search algorithm and a procedure for the calculation of the resulting forces between the cable and the structure in case of a contact. The proposed algorithm is checked and verified by the simulation of a post-tensioning operation of a 2D truss structure. A practical application of the proposed scheme is presented by considering the strengthening of an existing structure as a case study.

#### **8.2 Conclusions**

A unified procedure based on contact mechanics is proposed for the solution of the interaction problem between multi-segment continuous cable and elastic structures. It

is implemented into a finite element code, tested and verified. It is shown that the procedure and the resulting tool is very convenient for the simulation of the post-tensioning process of structures using cables.

The proposed procedure has some comparative advantages over some alternative approaches readily available to engineers in the commercial finite element programs. First of all, it is natural and closely mimics the real-life application of the post-tensioning process in the field by shortening the unstressed length of the tensioning cable. It makes it possible for the engineer to observe the variation of the stresses in various parts of the structure in the course of the tensioning process. This is important because it is seen that some parts of the structure becomes temporarily overstressed although the resulting stresses at the end of the tensioning process are within the safe limits.

Another point is that, in the proposed procedure it is not necessary to define the initial geometry of the post-tensioning cable at the onset of the simulation process. Given the unstressed length and the location of its end points, it is started in its natural form since the form-finding step of the cable is an integral part of its equilibrium state. This is seen to be a major drawback in the use of the capabilities of the commercially available general-purpose finite element programs for the simulation of the post-tensioning process.

In an effort to verify the response of the structure during post-tensioning process predicted by the proposed algorithm, the same simulations are also performed using the general-purpose finite element program ANSYS for a number of cases. In practice, the post-tensioning of existing structures can be of two types. In one approach the ends of the tensioning cable are anchored on the structure itself. Consequently, the cable tension is transferred to the subject structure. This can be termed as a self-contained or free-standing or simply internal post-tensioning. In an alternative approach, the ends of the tensioning cable are grounded on another structure external to the subject structure. This way the cable tension is transferred to the other structure. This type of tensioning can be termed as external post-tensioning. Example simulations of both types are performed and the results are seen to be in a reasonably good agreement. Handling the internal type of post-tensioning is much easier and natural with the



proposed algorithm as opposed to using a general-purpose finite element program and as expected, an external type of post-tensioning is seen to be much more effective in the case of increasing the load carrying capacity of existing structures.



## REFERENCES

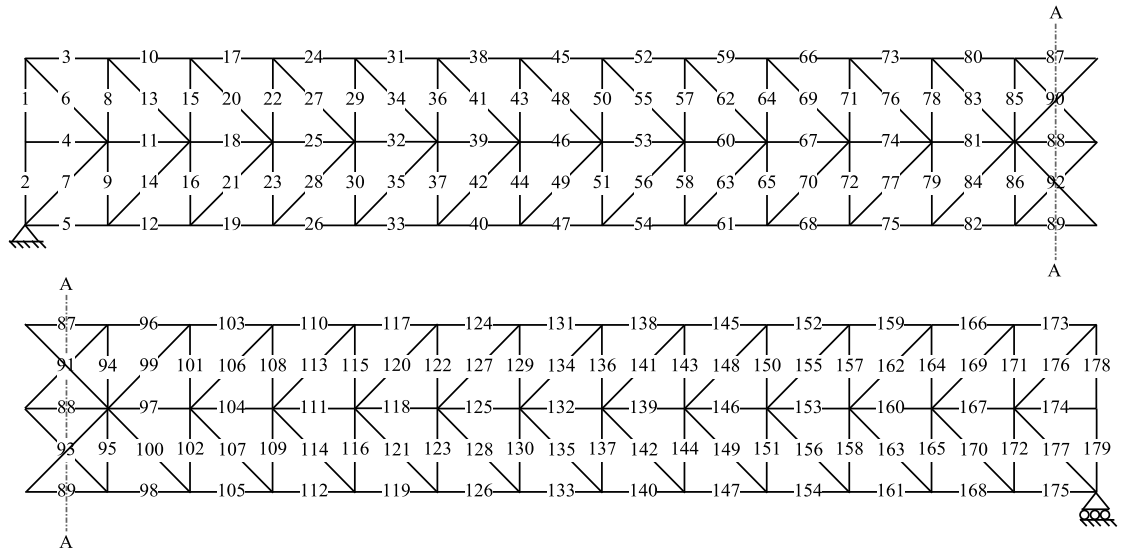
- [1] Ahmadizadeh, M.. (2013) Three-dimensional geometrically nonlinear analysis of slack cable structures. *Computers and Structures*, 128, 160-169.
- [2] Andreu, A., Gil, L., Roca, P.. (2006). A new deformable catenary element for the analysis of cable net structures. *Computers & Structures*, 84, 1882-1890.
- [3] Aufaure, M.. (1993). A finite element of cable passing through a pulley. *Computers & Structures*, 46, 807-812.
- [4] Aufaure, M.. (2000). A three-node cable element ensuring the continuity of the horizontal tension; a clamp-cable element. *Computers & Structures*, 74, 243-251.
- [5] Bathe, K.-J., Chaudhary, A.. (1985). A solution method for planar and axisymmetric contact problems. *International Journal for Numerical Methods in Engineering*, 21, 65-88.
- [6] Bathe, K.-J., (1996). *Finite Element Procedures in Engineering Analysis*, Prentice-Hall, New Jersey, USA.
- [7] Bruno, D., Leonardi, A.. (1999). Nonlinear structural models in cableway transport systems. *Simulation Practice and Theory*, 7, 207-218.
- [8] Chawla V., Laursen, T.A.. (1998). Energy consistent algorithms for frictional contact problems. *International Journal for Numerical Methods in Engineering*, 42, 799-827.
- [9] Chue S.-H.. (1983). Mechanics of static catenary with current loading. *Journal of Waterway Port Coastal Ocean Engineering*, 109, 340-349.
- [10] Demir, A.. (2011). *Form finding and structural analysis of cables with multiple supports*, M.S. thesis, Middle East Technical University, Ankara, Turkey.
- [11] Der Kiureghian, A., Sackman, J.L.. (2005). Tangent geometric stiffness of inclined cables under self-weight. *Journal of Structural Engineering ASCE*, 131, 941-945.
- [12] Deufhard, P., Krause, R., Ertel, S.. (2008). A contact-stabilized Newmark method for dynamical contact problems. *International Journal for Numerical Methods in Engineering*, 73, 1274-1290.

- [13]Dishinger, F.. (1949). Hängebrücken für Schwere Verkehrslasten. *Der Bauingenieur*, 24, 65-107.
- [14]Ernst, H.J.. (1965). Der E-Modul von Seilen unter Berücksichtigung des Durchhangers. *Der Bauingenieur*, 40(2), 52-55.
- [15]Feng, Z.-Q., Magnain, B., Cros, J.-M.. (2006). Solution of large deformation impact problems with friction between Blatz-Ko hyperelastic bodies. *International Journal of Engineering Science*, 44, 113-126.
- [16]Feng, Z.-Q., Peyraut, F., Labed, N.. (2003). Solution of large deformation contact problems with friction between Blatz-Ko hyperelastic bodies. *International Journal of Engineering Science*, 41, 2213-2226.
- [17]Feng, Z.-Q.. (1995). 2D or 3D frictional contact algorithms and applications in a large deformation context. *Communications in Numerical Methods in Engineering*, 11, 409-416.
- [18]Fleming, J.F.. (1979). Nonlinear static analysis of cable-stayed bridge structures. *Computers & Structures*, 10, 621-635.
- [19]Fujun W., Jiangang, C., Zhenhan, Y.. (2000). A contact searching algorithm for contact-impact problems. *ACTA Mechanica Sinica*, 16(4), 374-382.
- [20]Greco, L., Impollonia, N., Cuomo, M.. (2014). A procedure for the static analysis of cable structures following elastic catenary theory. *International Journal of Solids and Structures*, 51, 1521-1533.
- [21]Hajdin, N., Michaltsos, G.T., Konstantakopoulos, T.G.. (1998). About the equivalent modulus of elasticity of cables of cable-stayed bridges. *Sci. J. Facta Universitatis Arc and Civil Eng. Series*, 1(5), pp. 569-575.
- [22]Hughes, T.J.R., Taylor R.L., Kanoknukulchai, W.. (1977). *A finite element method for large displacement contact and impact problems in Formulations and Computational Algorithms in Finite Element Analysis*, M.I.T. Press.
- [23]Hughes, T.J.R., Taylor, R.L., Sackman, J.L.. (1974). *Finite element formulation and solution of contact-impact problems in continuum mechanics*, SESM Report No. 74-3, University of California, Berkeley.
- [24]Hughes, T.J.R., Taylor, R.L., Sackman, J.L.. (1975). *Finite element formulation and solution of contact-impact problems in continuum mechanics - II*, SESM Report No. 75-3, University of California, Berkeley.
- [25]Hughes, T.J.R., Taylor, R.L., Sackman, J.L.. (1975). *Finite element formulation and solution of contact-impact problems in continuum mechanics - III*, SESM Report No. 75-7, University of California, Berkeley.
- [26]Impollonia, N., Ricciardi, G., Saitta, F.. (2011). Statics of elastic cables under 3D point forces. *International Journal of Solids and Structures*, 48, 1268-1276.

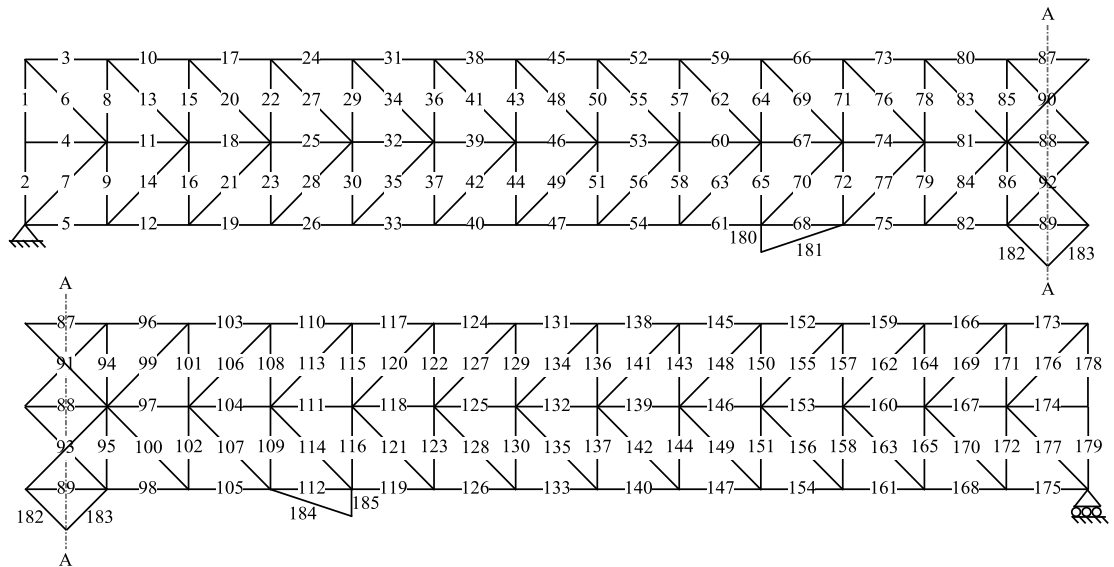
- [27] Khenous, H.B., Laborde, P., Yves, R.. (2006). Comparison of two approaches for the discretization of elastodynamic contact problems. *C.R. Acad. Sci. Paris*, 342, 791-796.
- [28] Laursen, L.A., Chawla, V.. (1997). Design of energy conserving algorithms for frictionless dynamic contact problems. *International Journal for Numerical Methods in Engineering*, 40, 863-886.
- [29] McDevitt, T.W., Laursen, T.A.. (2000). A mortar-finite element formulation for frictional contact problems. *International Journal for Numerical Methods in Engineering*, 48, 1525-1547.
- [30] McDonald B.M., Peyrot, A.H.. (1988). Analysis of cables suspended in sheaves. *Journal of Structural Engineering*, 114, 693-706.
- [31] McDonald B.M., Peyrot, A.H.. (1990). Sag tension calculations valid for any line geometry. *Journal of Structural Engineering*, 116, 2374-2386.
- [32] Micholas, J., Brinstiel, C.. (1962). Movements of cables due to changes in loading. *Transactions ASCE*, 127, 267-303.
- [33] Mostafa, S.A.A., Ahmad, S., Vahab, E., Alireza, N.R.. (2013). Nonlinear analysis of cable structures under general loadings. *Finite Elements in Analysis and Design*, 73, 11-19.
- [34] Peyrot, A.H., Goulois, A.M.. (1979). Analysis of cable structures. *Computers & Structures*, 10, 805-813.
- [35] Polat, M.U.. (1981). *Nonlinear Computer Analysis of Guyed Towers and Cables*, M.S. thesis, Middle East Technical University, Ankara, Turkey.
- [36] Ren, W.-X., Huang, M.-G., Hu, W.-H.. (2008). A parabolic cable element for static analysis of cable structures. *Engineering Computations, International Journal of Computer-Aided Engineering and Software*, 25(4), 366-384.
- [37] Santos, H.A.F.A., Paulo, C.I.A.. (2011). On a pure complementary energy principle and a force-based finite element formulation for non-linear elastic cables. *International Journal of Non-Linear Mechanics*, 46, 395-406.
- [38] Schreppers, G.J.M.A., Brekelmans, W.A.M., Sauren, A.A.H.J.. (1992). A finite element formulation of the large sliding contact. *International Journal for Numerical Methods in Engineering*, 35, 133-143.
- [39] Skop, R.A., O'Hara, G.J.. (1970). The Method of Imaginary Reactions : A New Technique for Analyzing Structural Cable Systems. *Marine Technology Society Journal*, 4, 21-30.
- [40] Such, M., Jimenez-Octavio, J.R., Carnicero, A., Lopez-Garcia, O.. (2009). An approach based on the catenary equation to deal with static analysis of three dimensional cable structures. *Engineering Structures*, 31, 2162-2170.

- [41] Taylor, R.L., Papadopoulos, P.. (1993). On a finite element method for dynamic contact/impact problems. *International Journal for Numerical Methods in Engineering*, 36, 2123-2140.
- [42] Wang C.-M., Jin, D.. (1989). Basic problem on optimal spatial cable layout. *Journal of Engineering Mechanics*, 115, 1115-1120.
- [43] Wang C.-M.. (1984). Optimal shape of cables. *Journal of Engineering Mechanics*, 110, 1649-1653.
- [44] Zhou, B., Accorsi, M.L., Leonard, J.W.. (2004). Finite element formulation for modelling sliding cable elements. *Computers & Structures*, 82, 271-280.

## APPENDIX



Appendix 1 Element labels of the original truss structure



Appendix 2 Element labels of the truss structure after modification

### Appendix 3 Element types of truss system

Element Number	Type	Element Number	Type	Element Number	Type	Element Number	Type	Element Number	Type
1	4	38	1	75	2	112	2	149	4
2	4	39	3	76	5	113	5	150	4
3	1	40	2	77	5	114	5	151	4
4	3	41	4	78	5	115	5	152	1
5	2	42	4	79	5	116	5	153	3
6	4	43	5	80	1	117	1	154	2
7	4	44	5	81	3	118	3	155	4
8	4	45	1	82	2	119	2	156	4
9	4	46	3	83	5	120	5	157	4
10	1	47	2	84	5	121	5	158	4
11	3	48	5	85	5	122	5	159	1
12	2	49	5	86	5	123	5	160	3
13	4	50	5	87	1	124	1	161	2
14	4	51	5	88	3	125	3	162	4
15	4	52	1	89	2	126	2	163	4
16	4	53	3	90	5	127	5	164	4
17	1	54	2	91	5	128	5	165	4
18	3	55	5	92	5	129	5	166	1
19	2	56	5	93	5	130	5	167	3
20	4	57	5	94	5	131	1	168	2
21	4	58	5	95	5	132	3	169	4
22	4	59	1	96	1	133	2	170	4
23	4	60	3	97	3	134	5	171	4
24	1	61	2	98	2	135	5	172	4
25	3	62	5	99	5	136	5	173	1
26	2	63	5	100	5	137	5	174	3
27	4	64	5	101	5	138	1	175	2
28	4	65	5	102	5	139	3	176	4
29	4	66	1	103	1	140	2	177	4
30	4	67	3	104	3	141	4	178	4
31	1	68	2	105	2	142	4	179	4
32	3	69	5	106	5	143	4	180	5
33	2	70	5	107	5	144	4	181	5
34	4	71	5	108	5	145	1	182	5
35	4	72	5	109	5	146	3	183	5
36	4	73	1	110	1	147	2	184	5
37	4	74	3	111	3	148	4	185	5



#### Appendix 4 Properties of element types

Name	Outer Diameter (mm)	Inner Diameter (mm)	Area (mm <sup>2</sup> )
Type1	219.1	195.1	7807.49
Type2	219.1	199.1	6569.07
Type3	88.9	80.9	1066.88
Type4	139.7	127.7	2520.19
Type5	139.7	131.7	1705.26

Appendix 5 Resultant stresses of elements for initial case

Element Number	Stress (MPa)	Element Number	Stress (MPa)	Element Number	Stress (MPa)	Element Number	Stress (MPa)	Element Number	Stress (MPa)
1	-61.3	37	32.7	73	-173.8	109	13.2	145	-112.9
2	-61.5	38	-128.6	74	16.4	110	-169.0	146	8.2
3	-26.2	39	10.0	75	203.2	111	14.6	147	132.8
4	-0.1	40	151.1	76	26.3	112	198.3	148	66.9
5	33.6	41	58.5	77	-22.9	113	37.5	149	-65.9
6	97.4	42	-57.4	78	-22.4	114	-36.1	150	-45.1
7	-103.4	43	-52.6	79	4.4	115	-33.1	151	37.5
8	-60.5	44	41.6	80	-177.0	116	20.6	152	-94.9
9	50.3	45	-142.0	81	20.8	117	-162.2	153	5.8
10	-51.8	46	11.8	82	204.8	118	13.6	154	111.8
11	-12.0	47	166.9	83	17.6	119	190.5	155	75.6
12	61.8	48	73.7	84	-7.2	120	49.4	156	-74.2
13	95.4	49	-72.9	85	13.8	121	-48.5	157	-49.7
14	-88.4	50	-46.2	86	-34.2	122	-39.6	158	42.3
15	-54.7	51	34.6	87	-168.3	123	27.6	159	-74.6
16	46.7	52	-153.2	88	16.7	124	-153.2	160	1.3
17	-74.6	53	12.6	89	191.5	125	12.6	161	88.1
18	1.3	54	180.0	90	-48.2	126	180.0	162	84.6
19	88.1	55	61.6	91	-48.2	127	61.6	163	-82.2
20	84.6	56	-60.7	92	61.6	128	-60.7	164	-54.7
21	-82.2	57	-39.6	93	61.6	129	-46.2	165	46.7
22	-49.7	58	27.6	94	13.8	130	34.6	166	-51.8
23	42.3	59	-162.2	95	-34.2	131	-142.0	167	-12.0
24	-94.9	60	13.6	96	-177.0	132	11.8	168	61.8
25	5.8	61	190.5	97	20.8	133	166.9	169	95.4
26	111.8	62	49.4	98	204.8	134	73.7	170	-88.4
27	75.6	63	-48.5	99	17.6	135	-72.9	171	-60.5
28	-74.2	64	-33.1	100	-7.2	136	-52.6	172	50.3
29	-45.1	65	20.6	101	-22.4	137	41.6	173	-26.2
30	37.5	66	-169.0	102	4.4	138	-128.6	174	-0.1
31	-112.9	67	14.6	103	-173.8	139	10.0	175	33.6
32	8.2	68	198.3	104	16.4	140	151.1	176	97.4
33	132.8	69	37.5	105	203.2	141	58.5	177	-103.4
34	66.9	70	-36.1	106	26.3	142	-57.4	178	-61.3
35	-65.9	71	-27.0	107	-22.9	143	-40.4	179	-61.5
36	-40.4	72	13.2	108	-27.0	144	32.7		

Appendix 6 Resultant stresses of elements for case 1 without snow load

Element Number	Stress (MPa)	Element Number	Stress (MPa)	Element Number	Stress (MPa)	Element Number	Stress (MPa)	Element Number	Stress (MPa)
1	-107.5	38	-30.1	75	-204.5	112	-202.0	149	100.5
2	-107.7	39	-95.7	76	-36.9	113	-24.4	150	52.4
3	-147.5	40	-185.6	77	9.7	114	15.2	151	-54.5
4	0.0	41	-13.6	78	38.2	115	11.1	152	-59.9
5	-38.0	42	2.5	79	11.8	116	-15.5	153	-102.7
6	-166.8	43	5.3	80	4.8	117	-19.6	154	-147.4
7	118.9	44	-8.6	81	-161.7	118	-111.0	155	-95.5
8	75.6	45	-27.6	82	-200.3	119	-198.7	156	96.2
9	-83.4	46	-117.6	83	-73.2	120	-24.4	157	51.3
10	-110.1	47	-189.5	84	-19.2	121	22.6	158	-52.2
11	-94.5	48	-13.7	85	15.5	122	11.2	159	-85.5
12	-86.7	49	18.2	86	18.5	123	-11.3	160	-107.6
13	-139.3	50	8.4	87	10.7	124	-24.1	161	-116.7
14	152.7	51	-9.8	88	-118.0	125	-111.7	162	-91.5
15	49.2	52	-24.1	89	-167.1	126	-193.8	163	94.1
16	-51.1	53	-111.7	90	-32.4	127	-19.4	164	49.2
17	-85.5	54	-193.8	91	-32.4	128	20.0	165	-51.1
18	-107.6	55	-19.4	92	-93.0	129	8.4	166	-110.1
19	-116.7	56	20.0	93	-93.0	130	-9.8	167	-94.5
20	-91.5	57	11.2	94	15.5	131	-27.6	168	-86.7
21	94.1	58	-11.3	95	18.5	132	-117.6	169	-139.3
22	51.3	59	-19.6	96	4.8	133	-189.5	170	152.7
23	-52.2	60	-111.0	97	-161.7	134	-13.7	171	75.6
24	-59.9	61	-198.7	98	-200.3	135	18.2	172	-83.4
25	-102.7	62	-24.4	99	-73.2	136	5.3	173	-147.5
26	-147.4	63	22.6	100	-19.2	137	-8.6	174	0.0
27	-95.5	64	11.1	101	38.2	138	-30.1	175	-38.0
28	96.2	65	-15.5	102	11.8	139	-95.7	176	-166.8
29	52.4	66	-15.2	103	-8.5	140	-185.6	177	118.9
30	-54.5	67	-113.5	104	-125.6	141	-13.6	178	-107.5
31	-33.7	68	-202.0	105	-204.5	142	2.5	179	-107.7
32	-101.5	69	-24.4	106	-36.9	143	6.0	180	-8.13
33	-179.4	70	15.2	107	9.7	144	-104.2	181	-1.49
34	-97.3	71	18.1	108	18.1	145	-33.7	182	-60.7
35	100.5	72	-4.4	109	-4.4	146	-101.5	183	-60.7
36	6.0	73	-8.5	110	-15.2	147	-179.4	184	-1.49
37	-104.2	74	-125.6	111	-113.5	148	-97.3	185	-8.13

Appendix 7 Resultant stresses of elements for case 1 with snow load

Element Number	Stress (MPa)	Element Number	Stress (MPa)	Element Number	Stress (MPa)	Element Number	Stress (MPa)	Element Number	Stress (MPa)
1	-201.5	38	-181.6	75	-18.1	112	-19.6	149	47.5
2	-201.7	39	-104.2	76	-14.5	113	14.0	150	10.5
3	-208.0	40	-53.3	77	-14.9	114	-24.2	151	-25.0
4	-0.3	41	51.0	78	19.2	115	-27.4	152	-179.3
5	-8.3	42	-63.4	79	18.7	116	-0.1	153	-117.7
6	-92.8	43	-56.8	80	-194.0	117	-206.8	154	-52.6
7	27.9	44	36.2	81	-172.9	118	-118.6	155	-30.5
8	21.3	45	-193.9	82	-11.5	119	-24.8	156	32.6
9	-46.2	46	-128.8	83	-70.1	120	24.7	157	3.7
10	-191.4	47	-39.9	84	-30.6	121	-25.8	158	-16.8
11	-128.0	48	68.1	85	32.7	122	-33.4	159	-187.4
12	-35.6	49	-62.0	86	-18.4	123	16.1	160	-128.9
13	-61.7	50	-45.1	87	-176.9	124	-202.3	161	-42.2
14	85.5	51	26.4	88	-124.0	125	-120.7	162	-15.1
15	-4.5	52	-202.3	89	15.1	126	-30.4	163	20.7
16	-10.3	53	-120.7	90	-94.1	127	46.0	164	-4.5
17	-187.4	54	-30.4	91	-94.1	128	-44.3	165	-10.3
18	-128.9	55	46.0	92	-43.4	129	-45.1	166	-191.4
19	-42.2	56	-44.3	93	-43.4	130	26.4	167	-128.0
20	-15.1	57	-33.4	94	32.7	131	-193.9	168	-35.6
21	20.7	58	16.1	95	-18.4	132	-128.8	169	-61.7
22	3.7	59	-206.8	96	-194.0	133	-39.9	170	85.5
23	-16.8	60	-118.6	97	-172.9	134	68.1	171	21.3
24	-179.3	61	-24.8	98	-11.5	135	-62.0	172	-46.2
25	-117.7	62	24.7	99	-70.1	136	-56.8	173	-208.0
26	-52.6	63	-25.8	100	-30.6	137	36.2	174	-0.3
27	-30.5	64	-27.4	101	19.2	138	-181.6	175	-8.3
28	32.6	65	-0.1	102	18.7	139	-104.2	176	-92.8
29	10.5	66	-209.3	103	-206.7	140	-53.3	177	27.9
30	-25.0	67	-120.1	104	-133.8	141	51.0	178	-201.5
31	-167.9	68	-19.6	105	-18.1	142	-63.4	179	-201.7
32	-113.6	69	14.0	106	-14.5	143	-40.8	180	-15.3
33	-67.8	70	-24.2	107	-14.9	144	-91.3	181	-6.96
34	-42.6	71	-11.7	108	-11.7	145	-167.9	182	-80
35	47.5	72	8.8	109	8.8	146	-113.6	183	-80
36	-40.8	73	-206.7	110	-209.3	147	-67.8	184	-6.96
37	-91.3	74	-133.8	111	-120.1	148	-42.6	185	-15.3

Appendix 8 Resultant stresses of elements for case 2 without snow load

Element Number	Stress (MPa)	Element Number	Stress (MPa)	Element Number	Stress (MPa)	Element Number	Stress (MPa)	Element Number	Stress (MPa)
1	-90.4	38	-16.0	75	-197.4	112	-195.0	149	96.6
2	-90.6	39	-85.5	76	-35.3	113	-22.5	150	50.2
3	-130.0	40	-178.6	77	10.8	114	14.3	151	-52.4
4	-0.3	41	-13.0	78	35.6	115	10.1	152	-42.9
5	-35.5	42	2.1	79	9.5	116	-14.3	153	-92.3
6	-159.2	43	4.9	80	17.2	117	-5.2	154	-143.8
7	117.7	44	-8.2	81	-146.2	118	-100.2	155	-91.7
8	73.4	45	-13.6	82	-194.1	119	-191.9	156	92.4
9	-80.7	46	-106.9	83	-68.5	120	-22.3	157	49.2
10	-93.6	47	-182.4	84	-15.0	121	20.7	158	-50.0
11	-82.2	48	-13.1	85	11.8	122	10.0	159	-67.5
12	-82.7	49	17.4	86	16.3	123	-10.2	160	-96.5
13	-135.3	50	8.0	87	21.9	124	-9.2	161	-114.3
14	148.0	51	-9.5	88	-106.4	125	-101.1	162	-87.8
15	47.7	52	-10.2	89	-162.4	126	-187.4	163	90.1
16	-49.4	53	-101.1	90	-25.3	127	-17.4	164	47.2
17	-69.8	54	-186.5	91	-25.9	128	18.0	165	-48.8
18	-96.9	55	-18.8	92	-87.6	129	7.2	166	-91.1
19	-111.8	56	19.4	93	-88.2	130	-8.7	167	-82.9
20	-88.7	57	10.7	94	11.5	131	-12.4	168	-85.6
21	91.2	58	-11.0	95	16.8	132	-106.8	169	-135.0
22	49.7	59	-5.9	96	17.3	133	-183.5	170	146.8
23	-50.6	60	-100.3	97	-146.2	134	-11.7	171	73.2
24	-44.9	61	-191.3	98	-194.2	135	16.1	172	-80.1
25	-92.3	62	-23.7	99	-67.2	136	4.1	173	-127.4
26	-141.6	63	22.1	100	-16.3	137	-7.5	174	-0.2
27	-92.7	64	10.7	101	34.9	138	-14.5	175	-38.8
28	93.4	65	-15.2	102	10.2	139	-85.5	176	-158.7
29	50.8	66	-1.6	103	5.1	140	-180.1	177	116.8
30	-52.9	67	-102.5	104	-113.4	141	-12.1	178	-90.4
31	-19.5	68	-194.6	105	-197.7	142	1.3	179	-90.6
32	-91.2	69	-23.7	106	-34.1	143	5.1	180	-7.81
33	-172.7	70	15.4	107	9.4	144	-100.9	181	-1.63
34	-94.5	71	17.2	108	16.5	145	-17.8	182	-59.4
35	97.6	72	-5.0	109	-4.5	146	-91.2	183	-59
36	5.6	73	4.8	110	-1.1	147	-174.6	184	-2.61
37	-101.4	74	-113.5	111	-102.4	148	-93.5	185	-7.56

Appendix 9 Resultant stresses of elements for case 2 with snow load

Element Number	Stress (MPa)	Element Number	Stress (MPa)	Element Number	Stress (MPa)	Element Number	Stress (MPa)	Element Number	Stress (MPa)
1	-120.6	38	-174.8	75	4.8	112	2.0	149	39.6
2	-120.7	39	-91.9	76	-10.2	113	18.9	150	5.4
3	-191.4	40	-35.9	77	-15.7	114	-28.3	151	-20.7
4	-0.6	41	56.1	78	14.1	115	-31.3	152	-168.8
5	-4.2	42	-68.4	79	16.5	116	1.0	153	-104.6
6	-73.5	43	-61.6	80	-193.0	117	-202.9	154	-38.4
7	23.8	44	39.7	81	-154.1	118	-106.1	155	-22.1
8	16.3	45	-188.3	82	10.6	119	-4.1	156	23.9
9	-38.3	46	-116.3	83	-63.3	120	29.4	157	-1.7
10	-176.8	47	-21.2	84	-26.7	121	-30.1	158	-12.0
11	-98.4	48	74.5	85	29.2	122	-37.2	159	-174.7
12	-27.0	49	-68.4	86	-23.7	123	18.4	160	-112.6
13	-54.4	50	-49.3	87	-176.7	124	-197.5	161	-30.8
14	71.2	51	29.3	88	-109.7	125	-108.3	162	-6.7
15	-9.8	52	-197.7	89	34.8	126	-10.5	163	10.8
16	-4.8	53	-108.3	90	-90.1	127	51.6	164	-9.9
17	-175.0	54	-10.4	91	-90.2	128	-49.8	165	-4.8
18	-112.7	55	51.4	92	-33.2	129	-49.4	166	-176.5
19	-30.4	56	-49.6	93	-33.2	130	29.4	167	-98.4
20	-6.8	57	-37.1	94	29.2	131	-188.1	168	-27.3
21	10.9	58	18.3	95	-23.6	132	-116.3	169	-54.4
22	-1.7	59	-203.0	96	-193.0	133	-21.3	170	71.1
23	-12.1	60	-106.1	97	-154.1	134	74.7	171	16.3
24	-169.1	61	-4.0	98	10.6	135	-68.6	172	-38.2
25	-104.6	62	29.2	99	-63.1	136	-61.7	173	-191.1
26	-38.1	63	-29.9	100	-26.8	137	39.8	174	-0.6
27	-22.3	64	-31.3	101	14.0	138	-174.6	175	-4.6
28	24.1	65	0.9	102	16.6	139	-91.9	176	-73.5
29	5.5	66	-206.4	103	-204.5	140	-36.1	177	23.7
30	-20.7	67	-107.1	104	-119.6	141	56.2	178	-120.3
31	-159.7	68	2.1	105	4.8	142	-68.5	179	-120.5
32	-101.1	69	18.8	106	-10.1	143	-44.5	180	-16.5
33	-50.8	70	-28.1	107	-15.8	144	-86.3	181	-2.56
34	-35.0	71	-15.4	108	-15.4	145	-159.5	182	-79.1
35	39.8	72	10.0	109	10.1	146	-101.1	183	-79.1
36	-44.5	73	-204.5	110	-206.3	147	-51.0	184	-2.68
37	-86.4	74	-119.7	111	-107.1	148	-34.8	185	-16.4

Appendix 10 Resultant stresses of elements for case 3 without snow load

Element Number	Stress (MPa)	Element Number	Stress (MPa)	Element Number	Stress (MPa)	Element Number	Stress (MPa)	Element Number	Stress (MPa)
1	-72.0	38	105.3	75	-207.4	112	-202.7	149	97.9
2	-72.2	39	-28.7	76	-28.2	113	-20.7	150	50.5
3	-9.7	40	-187.3	77	17.2	114	16.8	151	-53.3
4	-0.4	41	-11.3	78	21.7	115	8.4	152	78.0
5	-42.5	42	0.1	79	-4.0	116	-14.0	153	-35.9
6	-150.6	43	2.7	80	131.1	117	114.4	154	-151.8
7	133.5	44	-7.2	81	-63.9	118	-43.3	155	-92.7
8	75.2	45	107.2	82	-209.3	119	-199.1	156	93.5
9	-82.9	46	-50.8	83	-44.9	120	-20.0	157	49.6
10	27.5	47	-190.5	84	8.5	121	19.5	158	-50.8
11	-34.4	48	-10.4	85	-16.6	122	8.1	159	53.1
12	-90.9	49	15.0	86	7.9	123	-10.0	160	-40.5
13	-138.5	50	6.0	87	126.9	124	110.8	161	-122.0
14	151.8	51	-8.6	88	-44.0	125	-44.6	162	-88.8
15	47.8	52	110.1	89	-180.0	126	-194.9	163	91.3
16	-50.0	53	-44.6	90	23.7	127	-15.2	164	47.5
17	51.6	54	-194.3	91	23.4	128	16.3	165	-49.6
18	-40.8	55	-16.2	92	-74.8	129	5.5	166	29.2
19	-120.3	56	17.2	93	-75.2	130	-8.1	167	-34.9
20	-89.4	57	8.6	94	-16.8	131	108.0	168	-92.8
21	92.0	58	-10.4	95	8.3	132	-50.7	169	-138.3
22	50.0	59	113.9	96	131.2	133	-191.3	170	151.1
23	-51.2	60	-43.3	97	-63.9	134	-9.5	171	75.1
24	76.7	61	-198.7	98	-209.3	135	14.1	172	-82.5
25	-35.9	62	-20.9	99	-44.1	136	2.2	173	-7.9
26	-150.3	63	20.4	100	7.6	137	-6.8	174	-0.4
27	-93.3	64	8.9	101	21.2	138	106.3	175	-44.7
28	94.2	65	-14.6	102	-3.5	139	-28.7	176	-150.3
29	50.9	66	117.8	103	123.2	140	-188.3	177	132.9
30	-53.6	67	-44.0	104	-49.2	141	-10.7	178	-71.9
31	102.2	68	-202.5	105	-207.6	142	-0.5	179	-72.0
32	-34.7	69	-21.5	106	-27.3	143	3.6	180	-5.68
33	-181.7	70	17.5	107	16.3	144	-103.7	181	-4.95
34	-95.2	71	12.6	108	12.1	145	103.4	182	-60.5
35	98.5	72	-9.6	109	-9.3	146	-34.7	183	-60.3
36	3.9	73	122.9	110	118.2	147	-183.0	184	-5.6
37	-104.0	74	-49.3	111	-43.9	148	-94.6	185	-5.51

Appendix 11 Resultant stresses of elements for case 3 with snow load

Element Number	Stress (MPa)	Element Number	Stress (MPa)	Element Number	Stress (MPa)	Element Number	Stress (MPa)	Element Number	Stress (MPa)
1	-129.6	38	-134.4	75	147.6	112	142.8	149	2.6
2	-129.7	39	-20.9	76	17.6	113	55.9	150	-28.6
3	-78.7	40	59.7	77	-26.1	114	-60.8	151	-0.3
4	-1.6	41	116.9	78	-22.3	115	-70.5	152	-102.1
5	11.4	42	-131.9	79	1.3	116	9.6	153	-41.0
6	1.7	43	-122.3	80	-203.5	117	-196.0	154	26.8
7	-24.4	44	80.8	81	-51.5	118	-35.6	155	27.6
8	-26.9	45	-161.9	82	147.9	119	129.6	156	-24.3
9	-13.0	46	-50.9	83	-31.8	120	73.7	157	-41.5
10	-79.2	47	90.5	84	-1.3	121	-71.8	158	14.7
11	-46.3	48	151.5	85	1.8	122	-80.4	159	-94.6
12	3.3	49	-142.8	86	-71.8	123	40.8	160	-55.0
13	1.7	50	-101.3	87	-189.8	124	-182.5	161	19.1
14	25.5	51	61.3	88	-29.0	125	-39.9	162	54.7
15	-56.3	52	-182.3	89	165.5	126	114.1	163	-47.5
16	27.7	53	-39.9	90	-75.2	127	111.6	164	-56.2
17	-94.0	54	113.9	91	-75.1	128	-108.0	165	27.6
18	-54.9	55	111.9	92	25.1	129	-101.1	166	-79.8
19	18.5	56	-108.3	93	25.2	130	61.1	167	-46.2
20	54.9	57	-80.5	94	1.9	131	-162.2	168	3.9
21	-47.7	58	41.0	95	-71.9	132	-51.0	169	1.6
22	-41.6	59	-195.8	96	-203.5	133	90.8	170	25.8
23	14.8	60	-35.5	97	-51.5	134	151.2	171	-26.9
24	-101.6	61	129.5	98	147.9	135	-142.5	172	-13.1
25	-41.0	62	74.0	99	-32.0	136	-122.2	173	-79.3
26	26.3	63	-72.1	100	-1.0	137	80.6	174	-1.6
27	27.9	64	-70.7	101	-22.2	138	-134.7	175	12.2
28	-24.5	65	9.8	102	1.1	139	-20.9	176	1.6
29	-28.7	66	-206.0	103	-209.3	140	60.0	177	-24.2
30	-0.2	67	-33.3	104	-40.1	141	116.7	178	-129.9
31	-102.9	68	142.7	105	147.7	142	-131.7	179	-130.0
32	-34.5	69	56.1	106	17.3	143	-90.3	180	-25.2
33	25.6	70	-61.1	107	-25.8	144	-89.8	181	-2.92
34	4.7	71	-49.6	108	-49.5	145	-103.3	182	-106
35	2.4	72	14.8	109	14.6	146	-34.5	183	-106
36	-90.5	73	-209.2	110	-206.1	147	26.0	184	-2.7
37	-89.7	74	-40.0	111	-33.3	148	4.4	185	-25.2



## CURRICULUM VITAE



**Name** Dr. Abdullah Demir

**Date of Birth** 10.08.1985

**E-Mail** abdemir@metu.edu.tr

### **Education**

**Ph.D.** Middle East Technical University  
(2011-2017) Civil Engineering / Structural Mechanics

Thesis: Multi-Segment Continuous cables with frictional contact along their span.

**M. Sc.** Middle East Technical University  
(2009-2011) Civil Engineering / Structural Mechanics

Thesis: Form finding and structural analysis of cables with multiple supports.

**B. Sc.** Middle East Technical University  
(2006-2009) Civil Engineering

**B. Sc.** Middle East Technical University  
(2005-2006) Industrial Engineering

**B. Sc.** Middle East Technical University  
(2004-2005) Physics Engineering

## **Academic Titles**

**Research Assistant**  
(2009-2010)

Bartın University  
Civil Engineering

**Research Assistant**  
(2010-2017)

Middle East Technical University  
Civil Engineering / Structural Mechanics